

AD-A052 898

AIR FORCE INST OF TECH WRIGHT-PATTERSON AFB OHIO SCH--ETC F/8 14/2  
LONG PATH, VISIBLE AND INFRARED TRANSMISSOMETER: CALIBRATION AN--ETC(U)  
OCT 77 L O VROOMBOUT

UNCLASSIFIED

AFIT/6EP/PH/77-14

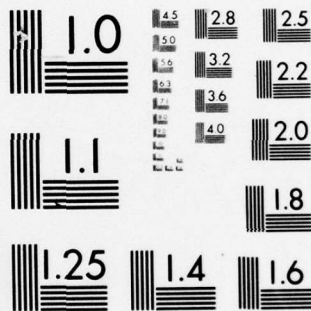
NL

| OF |

AD  
A052898



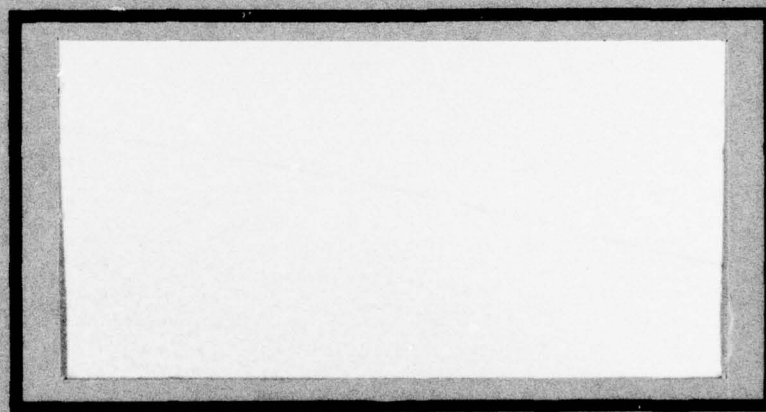
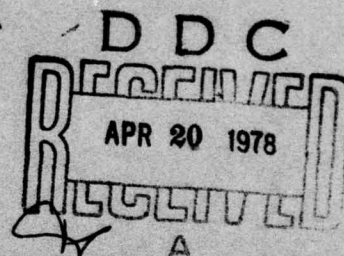
END  
DATE  
FILMED  
6 -78  
DDC



MICROCOPY RESOLUTION TEST CHART  
NATIONAL BUREAU OF STANDARDS-1963-A

AD No. ~~1~~  
DDC FILE COPY

AD A 052898



UNITED STATES AIR FORCE  
AIR UNIVERSITY  
AIR FORCE INSTITUTE OF TECHNOLOGY  
Wright-Patterson Air Force Base, Ohio

---

DISTRIBUTION STATEMENT A  
Approved for public release  
Distribution Unlimited

AD A 052898

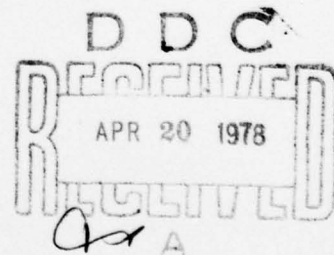
AD No. ~~1~~  
DDC FILE COPY

LONG PATH, VISIBLE AND INFRARED  
TRANSMISSOMETER: CALIBRATION AND USE

THESIS

AFIT/GEP/77-14

LEO O. VROOMBOUT



Approved for public release; distribution unlimited.

AFIT/GEP/PH/77-14

LONG PATH, VISIBLE AND INFRARED  
TRANSMISSOMETER: CALIBRATION AND USE

THESIS

Presented to the Faculty of the School of Engineering  
of the Air Force Institute of Technology  
Air University  
in Partial Fulfillment of the  
Requirements for the Degree of  
Master of Science

by  
Leo O. Vroombout  
Graduate Engineering Physics

October 1977

Approved for public release; distribution unlimited.

Acknowledgements

I would like to take this opportunity to express my appreciation to all those people in the Electro-Optics and Reconnaissance Branch of the Air Force Avionics Laboratory who helped me either directly or indirectly during the course of the work in this thesis. In particular, I wish to mention SSgt Roger J. Heinen, SSgt Donald O. Dumrauf and Sgt Donald Allen, all of Det 1, 2 Weather Squadron. Without their help, the experiment could never have been run. Also, thanks to Capt James D. Pryce who will have the job of the final calibration of the transmissometer and to Capt Edward H. Kelly, staff meteorologist, who, even though he couldn't clear up the weather, could at least tell me when it would be clear. Finally, most of all, thanks to my wife, Barbara Jean, who kept me moving even after the computer ate my permanent files.

Leo O. Vroombout

ACCESSION FOR	
WTS	Write Section <input checked="" type="checkbox"/>
DOC	Buff Section <input type="checkbox"/>
ORANNOUNCED	<input type="checkbox"/>
JUSTIFICATION	
BY	
DISTRIBUTION/AVAILABILITY ORDER	
Dist.	AVAIL. AND OF SPECIAL
A	

## Contents

	<u>Page</u>
Preface . . . . .	ii
List of Figures . . . . .	v
List of Tables . . . . .	vi
Abstract . . . . .	vii
I. Introduction . . . . .	1
Background . . . . .	1
Atmospheric Transmission . . . . .	2
Atmospheric Effects Measurement Program	3
Transmissometer Calibration . . . . .	4
Objectives . . . . .	5
II. Atmospheric Effects . . . . .	7
Atmospheric Attenuation Mechanisms . . . . .	7
Visible and Near-IR Region . . . . .	8
Far-IR Spectral Region . . . . .	9
Middle-IR Spectral Region . . . . .	9
LOWTRAN IIIB . . . . .	9
Modified LOWTRAN IIIB . . . . .	11
III. The Transmissometer . . . . .	12
General Description . . . . .	12
Theory . . . . .	13
Barnes Model 14-WP Transmissometer . . . . .	15
Installation . . . . .	18
Calibration . . . . .	18

## Contents

	<u>Page</u>
IV. The Experiment . . . . .	21
Weather Tower Effects . . . . .	21
Results . . . . .	21
Discussion . . . . .	27
Calibration Test . . . . .	30
Results . . . . .	30
Discussion . . . . .	42
V. Observations and Recommendations . . . . .	44
Observations . . . . .	44
Using the Transmissometer . . . . .	44
Calibration . . . . .	44
Recommendations . . . . .	45
Bibliography . . . . .	46
Appendix A: Source Listing: Modified LOWTRAN IIIB .	48
Appendix B: Draft Calibration Handbook . . . . .	62
Vita . . . . .	77

List of Tables

<u>Table</u>	<u>Page</u>
I. Transmissometer Beam Calculation Results . . . .	19
II. Weather Tower Effect Transmission Measurements .	26
III. Adjacent Window Measurements . . . . .	27
IV. Meteorological Conditions During Cal Test . . .	30
V. Spectral Transmission Data . . . . .	31

Abstract

The Barnes Model 14-WP transmissometer is one of the principle optical path calibration instruments of the Air Force Avionics Laboratory's Targeting Systems Characterization Facility. A simple test based on LOWTRAN IIIB was devised to certify system calibration while installed on an eight kilometer optical path. In addition, an optical path anomaly was investigated. Results are discussed and recommendations for additional calibration tests and new procedures are made.

LONG PATH, VISIBLE AND INFRARED  
TRANSMISSOMETER: CALIBRATION AND USE

I. Introduction

Background

During the war in Southeast Asia, it became more obvious than ever before that our forces must have the ability to prevent the enemy from taking advantage of darkness and adverse weather to move troops and supplies. One of the more successful sensors to be developed to satisfy this requirement was the Forward Looking Infrared set (FLIR). Although the FLIR concept had been demonstrated in the mid- 1950's, the electronics technology was not sufficiently developed to permit developing a useful, airborne FLIR until 1965 when the first exploratory development FLIR was tested in Southeast Asia. From then until 1974, over sixty different types of FLIR's were developed and several hundred were produced (Ref 11:5).

Throughout this period, the emphasis was on improving infrared (IR) detectors as well as the associated signal processing electronics and optics. However, by the end of this period, as cost increases began to exceed performance increases, the emphasis shifted toward better understanding of the physics of thermal imaging. Such improved understanding lead to computer modeling of the FLIR and its military appli-

cation. These models are intended to determine the extent to which FLIR performance must improve, if at all, in order to satisfy future military requirements. For instance, a major question to be answered prior to developing the next generation Air Force FLIR is what is the optimum spectral window for its operation? Does it fall within the 3 to 5 or 8 to 12 micrometer atmospheric windows? The models should answer this question. Unfortunately, there is little confidence in certain parts of the models; two particularly poor areas involve atmospheric propagation under very low visibility conditions and dynamic (search) modeling (Ref 23:2). This thesis will address the atmospheric propagation issue.

Atmospheric Transmission. The importance of atmospheric effects on the IR energy emitted by a target and received by a FLIR is well documented (Refs 1; 11:30-52; 12; 15; 22:10-16; 23: chap 3; 25: chap 6). The most important effects are (1) attenuation of the target energy by molecular absorption and by scattering out of the path, (2) scattering of background energy into the path, (3) the IR radiance of the air mass in the path, and (4) optical turbulence along the path.

The first three effects have been under study both in the laboratory and in the field since the late 1950's. In fact, in 1957, T. L. Altshuler (Ref 4) published a set of curves which may be used with reasonable confidence whenever the total transmission is greater than 20 percent. More recently, the laboratory and field data have been compiled and made available in the Air Force Geophysics Laboratory

computer program LOWTRAN (Refs 13; 17; 18; 19). It is generally agreed that the most recent version of LOWTRAN, LOWTRAN IIIIB (Ref 19), provides quite accurate transmission values when the total path transmission is greater than 10 per cent and scattering losses are low (Ref 23:1-13); however, when scattering losses are high, LOWTRAN departs from measured data by as much as a factor of three (Ref 16).

The fourth effect, optical turbulence, is the subject of current research (Refs 1; 2:31-35). As a result, only quasi-empirical mathematical models are available for engineering estimates of the degradation due to optical turbulence; these estimates do agree favorably with the limited experimental data that exist at this time (Ref 2:4).

This thesis will be concerned primarily with the first effect, attenuation by absorption and scattering. An overview of atmospheric transmission theory is provided in chapter II. Appendix A contains a computer listing of the modified LOWTRAN program developed for this thesis.

Atmospherics Effects Measurement Program. Because of the need to validate electro-optical sensor mathematical models and because of the lack of reliable atmospheric transmission data (Ref 11:31), particularly under low transmission/high scattering conditions, the Air Force Avionics Laboratory (AFAL) has established an Atmospheric Effects Measurement Program within its Targeting Systems Characterization Facility. This facility consists of electro-optical imaging sensors, including FLIR's, and test equipment, targets and mete-

orological instrumentation. The intent is to provide a fully characterized, eight kilometer, optical path between the sensors and the targets. To accomplish this, standard meteorological instruments as well as aerosol particle counting and sizing instruments are located at the zero, four and eight kilometer positions along the optical path. In addition, a Barnes Model 14-WP transmissometer (0.5 to 14 micrometers) is located so as to measure the spectral transmission along the eight kilometer path. The data from the transmissometer and the other instrumentation will provide the optical path calibration and will also be available to validate or to provide corrections to LOWTRAN. In the latter case, the transmissometer is the most important instrument; its calibration is one of the first tasks in the Atmospheric Effects Program and is the primary concern of this thesis. A summary of transmissometer theory is contained in chapter III.

Transmissometer Calibration. An IR transmissometer consists of a standard source of thermal radiation and a projector for that energy (somewhat like a searchlight) and a receiver that collects the energy after it has been attenuated by the atmosphere. The receiver electronics then convert the energy into a recordable output.

No standard procedure exists for calibrating a transmissometer; however, those procedures that do exist have several features in common. The receiver is first set up in the laboratory looking into its own source or at another black-body reference source. The electronics are then adjusted so

that a known relationship exists between this measurement and, based upon geometric arguments, that which would be expected on the test range. Then the transmissometer is installed and, if possible, some simple test is devised to verify the calibration *in situ*. This test usually consists of comparing the measured data to LOWTRAN predictions during periods of high transmission with low scattering (Refs 7:7).

In addition to transmissometer theory, chapter III also contains a description of the Barnes Model 14-WP transmissometer and of its installation in the AFAL Targeting Systems Characterization Facility. Chapter IV contains a description of the experiments performed with the transmissometer and the results. Chapter V contains a summary of the work under this thesis and recommendations for additional calibration testing. Appendix B is a draft calibration handbook for the transmissometer.

### Objectives

The objectives of the work described on this thesis were as follows:

- a. develop an understanding of the principles of operation of the transmissometer,
- b. devise a simple test to verify the transmissometer calibration while installed on the eight kilometer range,
- c. identify those areas which require additional calibration testing,
- d. conduct the initial transmission measurements

GEP/PH/77-14

prior to the transmissometer's being interfaced with the facility's automatic data processing equipment.

The last objective was not fulfilled partly because of equipment malfunction and partly because of visibilities that were too low to permit alignment and calibration.

## II. Atmospheric Effects

The atmosphere is important to all living creatures on this world not only because of the gases that are breathed and the rain and heat retention that are provided but also because of the protection from harmful solar radiation. None of these things could be provided if the atmosphere did not absorb electromagnetic radiation. As desirable as this feature is, it is undesirable to people or sensors that need to see through the atmosphere for long distances. Consequently, it is necessary to identify and quantify the atmospheric effects on electromagnetic radiation so that they at least might be corrected for. This chapter provides an overview of atmospheric attenuation mechanisms, a brief description of the most commonly accepted atmospheric transmission model and a brief description of a modification that was accomplished on that model for this thesis. Samples of the output of the model are included in the fourth chapter.

### Atmospheric Attenuation Mechanisms

As it propagates through the atmosphere, visible and infrared radiation are selectively absorbed by several atmospheric gases and scattered away from the direction of propagation by aerosol particles suspended in the atmosphere. Excellent summaries of these effects have been written by Hudson (Ref 9: chap. 4). Lloyd (Ref 11: chap. 2), and Wolfe (Ref 25: chap. 6). Middleton (Ref 15) has written an excellent reference text on seeing through the atmosphere and McCartney (Ref 12) has

discussed the scattering processes in great detail. The following discussion is drawn primarily from these sources.

The general process of attenuation of radiation as it passes through the atmosphere is called extinction. For monochromatic radiation, the transmittance along a path may be expressed by the Lambert-Beer law

$$T = \exp(-\sigma R) \quad (1)$$

where  $T$  is the transmittance,  $\sigma$  is the extinction coefficient and  $R$  is the length of the path. The extinction coefficient may be further separated into

$$\sigma = a + \gamma \quad (2)$$

where  $a$  is the absorption coefficient and  $\gamma$  is the scattering coefficient; both of these coefficients vary with wavelength. Absorption is primarily a function of molecular excitation and affects the infrared more than the visible spectral region. On the other hand, scattering is a function of particle size and, under most weather conditions, can cause greater attenuation in the visible than in the IR.

Visible and Near-IR Spectral Region. Extinction in this region is primarily caused by scattering by gas molecules (Rayleigh scattering) and haze (Mie scattering); however, water vapor molecular absorption does become important in the near-IR region. Energy scattered out of the path and then back again could also have an effect on transmission measurements. Such an effect should be very small if the

transmissometer receiver has a very small field of view. Stewart and Curcio (Ref 20:804) derived an equation for this effect

$$T_{\theta} = T + 0.5(1-T)(1-e^{-\theta}) \quad (3)$$

where  $T_{\theta}$  is the transmittance measured by an instrument having a field of view of  $\theta$  radians and  $T$  is the transmittance that would have been measured in the absence of scattered light. For fields of view smaller than one degree,  $T_{\theta}$  and  $T$  are the same except under conditions of very low transmission; i.e., less than three per cent.

Far-IR Spectral Region. Extinction in this region is primarily caused by molecular absorption. The most important absorbers are water vapor and carbon dioxide. Water vapor has both a discrete and a continuum absorption in this region. The latter is not well understood but has been measured. Scattering becomes the dominant extinction mechanism only for low visibility or for low temperature, low absolute humidity conditions.

Middle-IR Spectral Region. Extinction in this region is caused by both molecular absorption and scattering; however, there are discrete spectral regions (around 2.2 and 3.8 micrometers) in which transmission through haze is better than in the visible and transmission through water vapor is better than in the far-IR (Ref 2:6).

#### LOWTRAN IIIB

Because of the widely varying value of the extinction coefficient as a function of wavelength and even more so as a

function of atmospheric conditions (Pressure, temperature and absolute humidity), many attempts have been made to develop useable models for estimating atmospheric transmittance. Altshuler wrote one of the best early models (Ref 4); however, it was too cumbersome because of the use of scaled graphs. McClatchey et al, of the Air Force Geophysics Laboratory (formerly the Air Force Cambridge Research Laboratory), followed Altshuler's approach, added a lot of curve fitted empirical data (both laboratory and field measurements) and developed a very flexible computer model, which in its latest version, is called LOWTRAN IIIB (Ref 19). The code permits calculating atmospheric transmittance in the spectral region from 0.25 to 28.5 micrometers along arbitrary, slant paths. Any one of six standard atmospheric models may be used or meteorological or radiosonde data may be inserted. Five different aerosol models are also available; however, only the maritime model is said to compare favorably with measurements over the European continent during conditions of low visibility (Ref 16). In the absence of aerosol scattering, LOWTRAN's accuracy is stated to be within a few per cent (Ref 7).

LOWTRAN predicts atmospheric transmission by calculating the attenuation for each of the following contributors:

- a. water vapor line absorption ( $350-14500\text{cm}^{-1}$ )
- b. uniformly mixed gases ( $\text{CO}_2$ ,  $\text{N}_2\text{O}$ ,  $\text{CH}_4$ ,  $\text{CO}$ ,  $\text{N}_2$ , and  $\text{O}_2$ ) line absorption ( $500-8060$  and  $12970-13190\text{ cm}^{-1}$ )
- c. ozone line absorption ( $575-3270\text{ cm}^{-1}$ )
- d. nitrogen continuum ( $2080-2740\text{ cm}^{-1}$ )

- e. water vapor continuum ( $670-1400\text{ cm}^{-1}$ )
- f. molecular scattering ( $2740-40000\text{ cm}^{-1}$ )
- g. aerosol scattering and absorption ( $350-40000\text{ cm}^{-1}$ )
- h. ozone absorption ( $13000-23400\text{ cm}^{-1}$ )

The total transmittance for a  $20\text{ cm}^{-1}$  frequency interval is then obtained by multiplying the individual transmittances obtained from the above attenuations. This procedure is repeated throughout the spectral region of interest in increments of  $5\text{ cm}^{-1}$  or greater, as specified by the user. This approach has been shown to be valid for transmissions greater than about 30 per cent (Ref 23:24) and is probably valid down to about 10 per cent (Ref 23:1-14) provided that aerosol scattering is not the primary loss mechanism. Very little experimental data exists with which to correct or to validate LOWTRAN under low transmission/high scattering conditions.

#### Modified LOWTRAN IIIB

A substantial portion of the LOWTRAN IIIB program is concerned with computing transmission along slant paths. Since the optical path for this thesis is practically horizontal, these cards were removed. In order to increase the program's flexibility, several DO loops were added to permit iterating the temperature, dew point and visibility and plotting transmission as a function of the iterated variable or as a function of wavelength. A source listing is contained in appendix A.

### III. The Transmissometer

As mentioned in the first chapter, a transmissometer consists of a standard radiation source, a projector for that radiation and a receiver that collects the radiation after it has propagated through the atmosphere. This chapter provides a general description of an IR transmissometer, a brief description of the theory of its operation and a specific description of the transmissometer used for the work reported in this thesis, the Barnes Model 14-WP, and of its installation and calibration in the AFAL Targeting Systems Characterization Facility.

#### General Description

An IR transmissometer uses a high temperature black body as the source of its radiation. The source is usually maintained at a constant temperature by constant current electronics and its own thermal inertia. The radiation from the source floods an aperture which is located at the focal plane of the projector. In order to provide background discrimination, the energy is usually chopped at 1000Hz or more just in front of the aperture.

The projector is best compared to a searchlight, although, in essence, it is a collimator. The energy entering the aperture is collected by an off-axis paraboloid or by an on-axis paraboloid in a Newtonian configuration. The energy is then projected into the atmosphere in a highly collimated beam; the smaller the aperture, the greater the collimation.

For a true point source, the beam would be perfectly collimated.

After propagation through the atmosphere over a specified range, the beam is incident upon the receiver. The receiver optics, usually Cassegrainian, then focus the radiation upon a detector which is sensitive to IR energy in the wavelength region of interest. The wavelength region is normally defined by inserting a spectral filter in the optical path in front of the detector. The detector converts the IR energy into an electrical signal which is amplified and processed and then presented to the experimenter either as an irradiance value or as a transmission value. In the latter case, the transmission is defined to be the ratio of the IR energy actually collected to that IR energy which would have been collected if there were no intervening atmosphere. The next section details the procedure for calculating the energy that would have been collected in the absence of an atmosphere.

### Theory

One of the most comprehensive articles on beam projectors was written by Frank Benford in 1945 (Ref 5). Unfortunately, this article was only concerned with aspheric optics (the transmissometer used for this work had a spherical mirror). Klein (Ref 10:136-138) provides a reasonably detailed description of a searchlight using a spherical mirror as does Hudson (Ref 9:227-228). The following discussion is drawn from these sources.

Figure 1 shows a single mirror collimator/searchlight (source size and angles are exaggerated for clarity). The

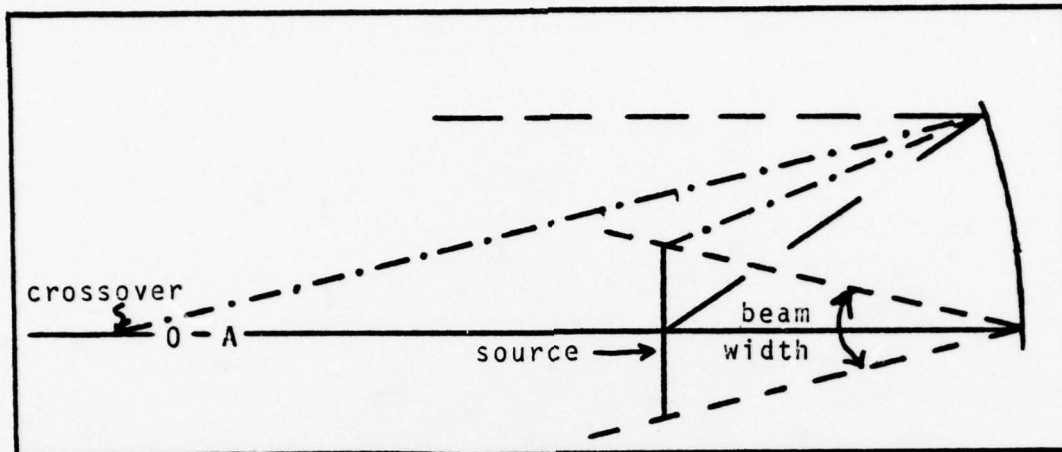


Fig. 1. Searchlight Ray Trace

limiting rays are depicted for bundles originating at the center and at one edge of the source. The angular beamwidth is equal to the ratio of the size of the source to the focal length of the mirror. The irradiance in the beam is independent of the distance from the mirror at all points in the central cone to the right of the crossover point. This occurs when the field point is close enough that the source aperture is the aperture stop. Beyond the crossover point, the irradiance in the beam falls off inversely with the square of the distance from the mirror provided that the field point is still in the central cone. In this case, the mirror is the aperture stop and increasing the source aperture size does not change the irradiance at the field point, only the beam diameter. The equations governing the irradiance at a field point in the central cone are, from Klein (Ref 10:137)

$$E_{\text{near}} = L\pi r_s^2 / f^2, \quad D < R_1 f / r_s \quad (4)$$

$$E_{\text{far}} = L \pi R_1^2 / D^2, \quad D \geq R_1 f / r_s \quad (5)$$

where

- E = irradiance (before or after crossover)
- L = radiance of the source
- $r_s$  = radius of the source aperture
- f = focal length of the mirror
- $R_1$  = radius of the mirror
- D = distance to the field point

Note that the distance from the mirror to the crossover point is  $R_1 f / r_s$  and that the beam angular width is  $2R_s / f$ . All of these equations are small angle approximations; this is justifiable since the angles involved typically range from a fraction to a few milliradians.

In practice, a source aperture should be selected such that the central cone diameter at the field point is large enough to compensate for beam wander induced by atmospheric turbulence/scintillation. Also, a very much smaller aperture,  $R_{\text{cal}}$ , should be selected for calibrating the receiver at zero range. This assures that the receiver electronics are not saturated as well as that the receiver is precisely aligned with the beam projector's optical axis. Then, using equations (4) and (5), the ratio of the calibration irradiance to the irradiance at the field point in the absence of the atmosphere is

$$\text{cal factor} = (R_{\text{cal}} D / R_1 f)^2 \quad (6)$$

#### Barnes Model 14-WP Transmissometer

Transmitter Assembly. The beam projector of the trans-

missometer used for this thesis consists of a Newtonian telescope, a Barnes 1000<sup>0</sup>C black body source and a tungsten foil 2820<sup>0</sup>K color temperature visible light source. Figure 2 is a layout drawing of these components. The radiation from the two sources is combined by a germanium beam splitter and is chopped by a gold plated mechanical chopper (1180Hz) prior to illuminating the aperture plate. The aperture plate is located at the focus of the telescope mirror and contains eight apertures ranging in size from 0.0048 inches in diameter (CAL) to 0.2560 inches in diameter. The telescope mirror has a focal length of 49.5 inches. Its diameter is 16.5 inches, but, allowing for obscuration, the effective diameter is 14.95 inches.

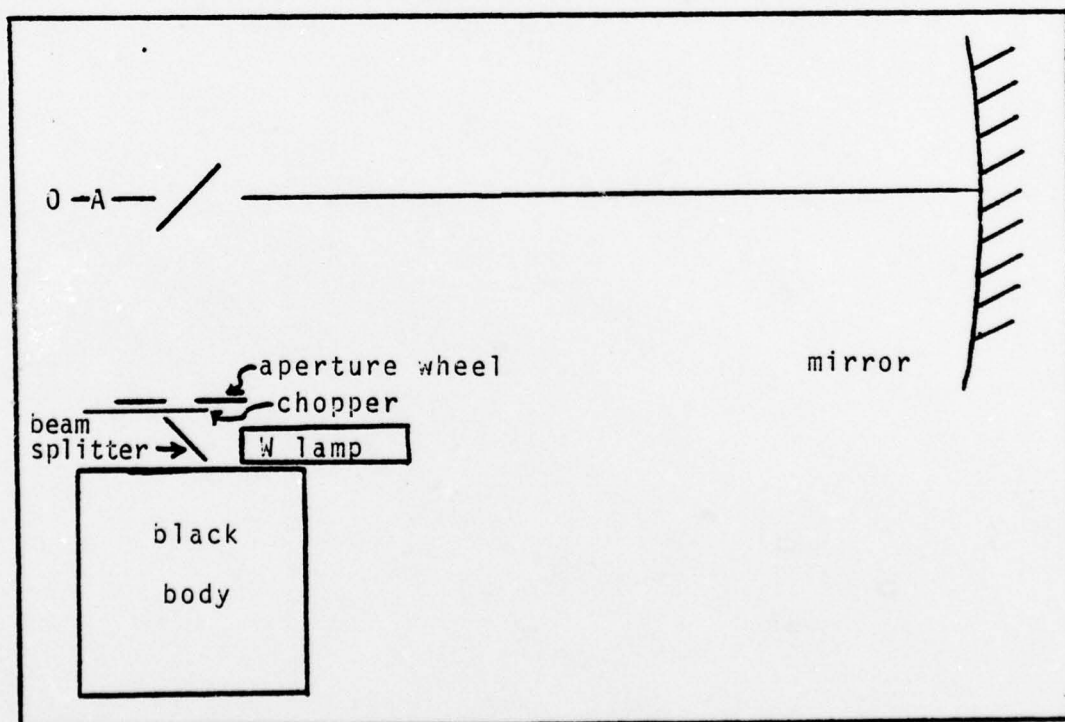


Fig. 2. Transmitter Assembly Layout

Receiver Assembly. The receiver assembly consists of a Cassegrainian telescope, a continuously variable filter (CVF) wheel, a detector and signal processing electronics. Figure 3 is a layout drawing of those components in the receiver head. Three different receiver assemblies are used to cover the spectral region from 0.5 to 14 micrometers; a silicon detector is used for the spectral region from 0.5 to 1.2 micrometers, an indium antimonide detector for 1.5 to 5.65 micrometers and a mercury cadmium telluride detector for 7.6 to 14.3 micrometers. The field of view of the receiver is 5 mrad for the visible receiver and 2.5 mrad for the IR receivers. The electrical signal from each receiver head is carried by cable to a separate electronics unit. Each electronics unit contains signal amplifiers, a narrow band filter assembly to

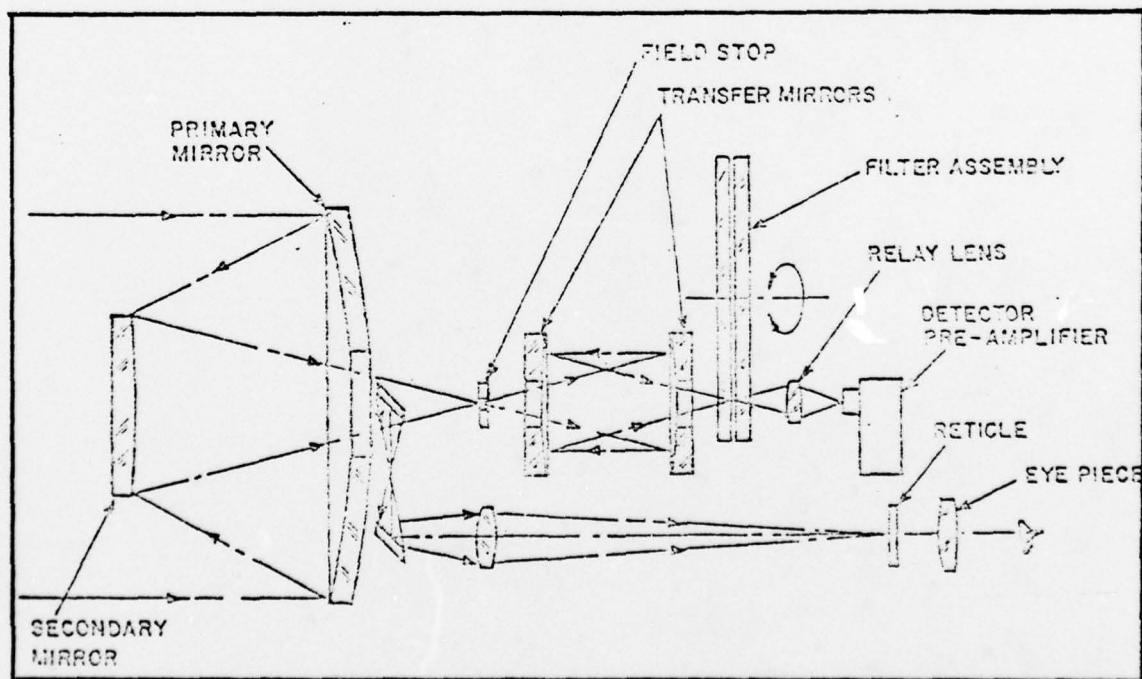


Fig. 3. Receiver Optical Layout

BEST AVAILABLE COPY

extract only the 1180Hz signal coming from the telescope, a phase lock loop to synchronize the receiver electronics with the telescope chopper, a digital meter and an analog meter to display the transmission reading, the filter wheel drive control and a binary coded digital output to provide transmission and filter wheel position data for computer input. During very low visibility conditions, synchronization may be achieved by telephone modem or by radio transmission and input of the synch signal generated by the telescope chopper.

#### Installation

The AFAL Targeting Systems Characterization Facility consists of laboratory rooms on the eleventh and twelfth floors of building 620 and a test area, the Trebein site, located five miles east of building 620. The transmitter assembly is installed in a building on the roof (fourteenth floor) of building 620. The receiver assemblies are located in a similar building at the Trebein site. The optical path is 7.944 kilometers long with an average elevation of 318 meters. Meteorological instrumentation is installed at building 620, at the Trebein site and on a tower located at the mid point of the optical path. During the course of the experiment, it was discovered that the weather tower interfered with the optical line of sight between the transmitter and receiver assemblies, and an additional objective of this thesis became to determine the effect of the weather tower on the beam.

#### Calibration

The transmissometer manufacturer provided the calibra-

tion data which is found herein in appendix B. Because of time constraints, it was necessary to accept this data and to install the transmissometer for test. Using the manufacturer's data and equations (4), (5) and (6), it is possible to determine the telescope's beam divergence, the distance to crossover, the size of the central cone at the Trebein site and the calibration factor. These are listed in Table I .

Table I

## Transmissometer Beam Calculation Results

Source Aperture Diameter (inch)	Divergence (mrad)	Crossover Distance (km)	Central Cone Diameter (m)
0.0048(CAL)	0.097	4.32	0.35
.0081	.164	2.56	0.88
.0141	.285	1.47	1.85
.0256	.517	0.810	3.69
.0444	0.897	.467	6.71
.0810	1.636	.256	12.6
0.1410	2.848	0.147	22.2
Calibration factor: 3.73 (range= 7.944 km)			

The manufacturer sent an engineer to Wright-Patterson to accomplish the initial calibration prior to installation. The calibration procedure detailed in appendix B was used with the calibration factor of 3.78 (value for 8km) for the peak response filter wheel position. All responses at other filter wheel positions were then determined and filter factors were calculated to normalize all readings to the peak response. The value of this technique is that no absolute

radiometric calibration is required. The limitations are the source output stability and optical transmission changes owing to dust deposits. As a result, periodic recalibration is required. Because of the difficulty of bringing the receiver assemblies to the transmitter assembly, an additional test is required to determine when recalibration is required. Developing this test is the principle objective of this thesis. It is discussed in the next chapter.

#### IV. The Experiment

As stated in chapter I, equipment malfunctions and uncooperative weather prevented satisfying the objective of conducting the initial transmission measurements as part of the Targeting Systems Characterization Facility program. Consequently, only the weather tower effects and the *in situ* calibration verification procedure/test were accomplished for this thesis. The work and the results are described in this chapter. Note: The transmissometer manufacturer refers to the InSB receiver as the near-Ir receiver; this erroneous labelling is also used in this thesis in order to avoid confusion.

##### Weather Tower Effects

Results. Initial alignment of the transmitter assembly could not be accomplished until 4 August 1977. Alignment was accomplished by removing the IR source and beam splitter (see figure 1) and looking through a microscope at the image in the plane of the source aperture. No alignment fixture was available; as a result, on-axis alignment was determined by lack of parallax and coma. The azimuth and elevation settings were then adjusted until the appropriate window of the Trebein building was in the center of the field of view; the receivers were located behind the second window from the north corner of the building; the transmitter was located behind the farthest south window of the small building on the top of the building 620 tower (see figure 5). Since electrical

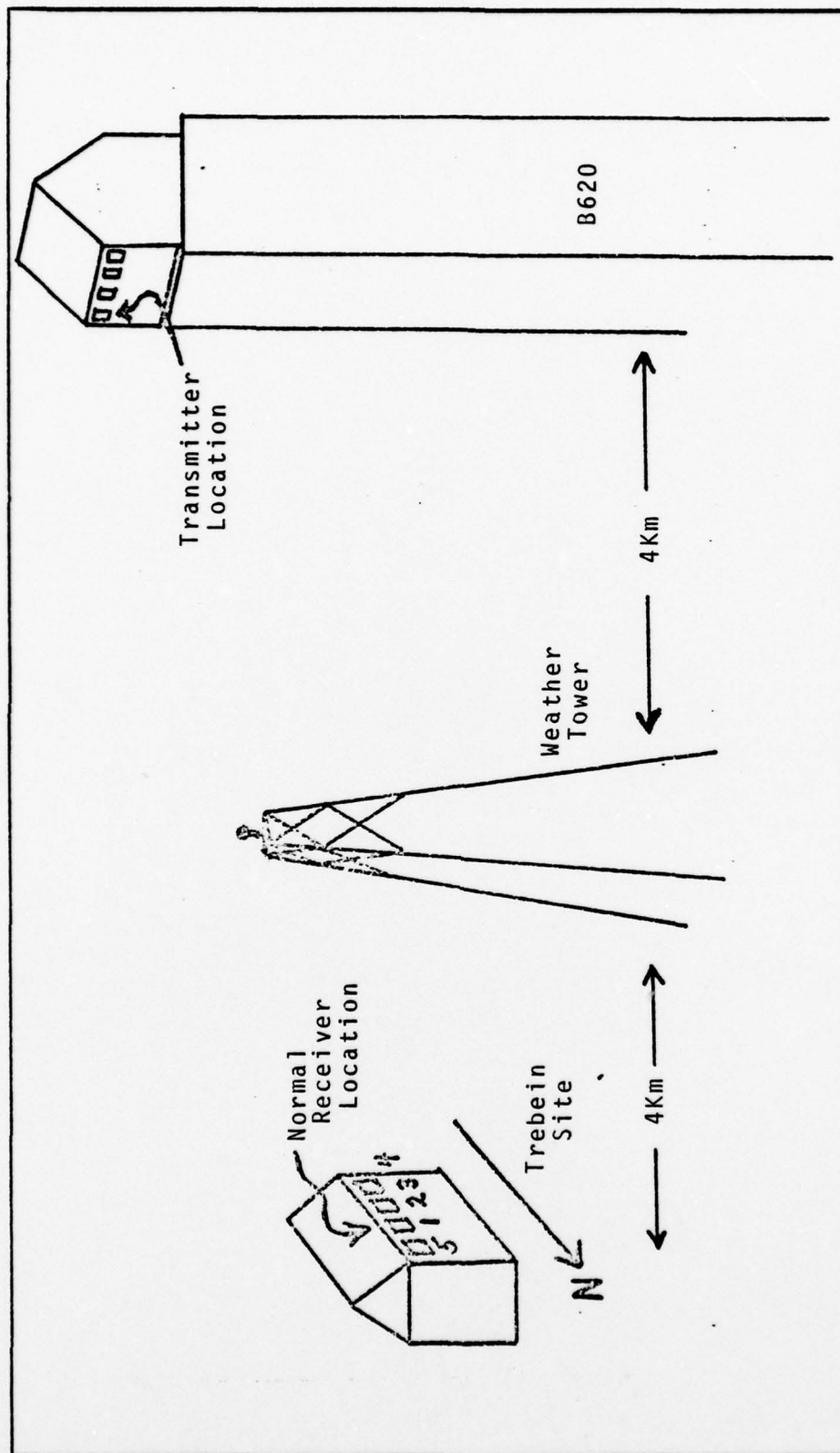


Fig. 4. Eight Kilometer Test Range.

power could not be applied to the transmitter assembly at that time, no tests were conducted until 11 and 12 August. Only the visible receiver could be used and it could not maintain phase lock with the incoming beam. After several days of troubleshooting, it became possible to conduct the following test on 18 and 19 August 1977.

The transmitter assembly was visually aligned with the appropriate window of the building at the Trebein site, and the receiver was then aligned by manually adjusting its line-of-sight until a maximum transmission reading was obtained. Then, the size of the transmitter's source aperture was varied. For each position of the aperture wheel, the transmission reading was recorded; since the readings were fluctuating rapidly, maximum and minimum values were estimated visually. Only the  $0.68\mu\text{m}$  position of the receiver filter wheel was used during this test. Next, the receiver was placed on a tripod in front of the next window (2) to the south, the transmitter assembly was aligned to that window and the experiment was repeated. A third set of measurements were also made for the last window to the south. The same sets of measurements were repeated the next day. The mean values of the data are depicted on figure 6 where the numbers 1, 2, and 3 refer to the receiver being located behind its normal window, the next one to the south and the last one to the south, respectively. The transmission readings were better on the first day because the visibility was about 20 miles on the first day and only 15 miles on the second day. Image boil (scintillation) hampered

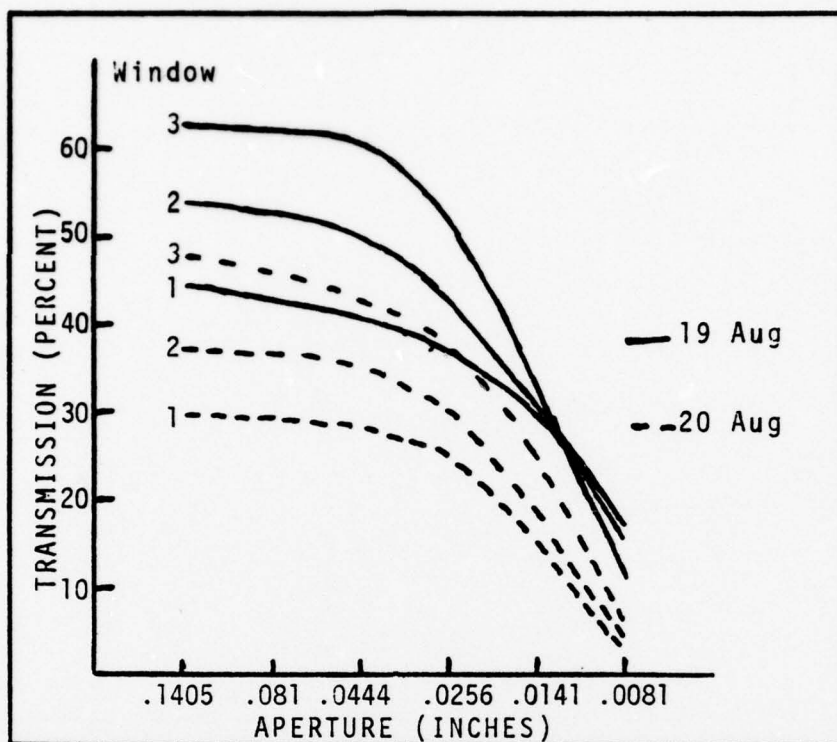


Fig. 5. Weather Tower Test Results, Day

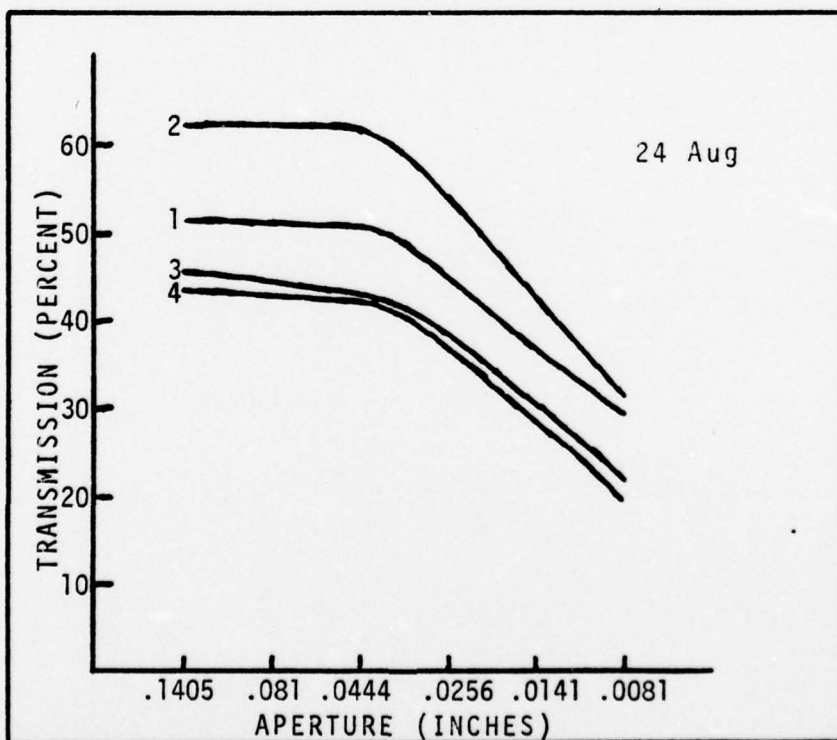


Fig. 6. Weather Tower Test Results, Night

the visual alignment and was greater on the first day than on the second day.

The higher transmission readings as the receiver was moved farther south were quite disturbing because the weather tower obstructed the line-of-sight to the normal window (1) only! Consequently, it was decided to repeat the experiments at night when atmospheric optical turbulence would be less and a more precise alignment could be assured. The experiment was repeated the night of 24 August 1977; this time a fourth test position was included, the stairs outside the south side of the building. The data are depicted in figure 7 and listed in table II. A flashlight located at the receiver was used to assure precise alignment of the transmitter assembly. This time the lowest transmission readings are those for the farthest south window (3) and the stairs (4) while the highest readings are still for the southern window (2) adjacent to the normal window (1). As a final check, these measurements were repeated the night of 22 September 1977. Since the visible receiver was not functioning this time, the near IR receiver was used; the filter wheel was stationary at  $2.19\mu\text{m}$ . These data are also included in table II; this time the northern window (5) adjacent to the normal window (1) was included. The measurements at the adjacent southern window (2) are still higher than for the other windows.

Additional information noted during these two tests:

1. As would be expected, based on the field of view plots in the manufacturer's calibration data, the transmission reading

Table II. Weather Tower Effect Transmission Measurements

Source Aperture Visible Transmission Reading 24 Aug 77

Diameter (inch)	Pos'n 1	Pos'n 2	Pos'n 3	Pos'n 4
0.1405	51.5±5.4**	61.9±4.5**	45.5±3.5	43.5±2.8
.0810	50.0±5.9	61.5±4.9	43.7±2.6	43.8±2.7
.0444	50.7±4.1	61.7±4.6	42.9±2.5	42.7±1.9
.0256	45.5±4.8	54.0±5.0	38.5±2.8	36.4±3.4
.0141	33.8±6.8	39.2±2.0	29.3±2.5	28.2±1.7
0.0081	29.2±2.2	31.7±2.0	22.1±1.8	17.0±3.0
Near IR Transmission Reading 22 Sep 77				
0.1405	19.8±2.4	37.2±4.8**	19.1±3.3	P
.0810	19.3±1.8	36.2±4.1	19.5±2.5	0
.0444	19.1±1.8	35.3±3.1	18.7±2.3	S
.0256	14.6±2.0	31.4±4.0	14.9±2.3	N
0.0141	9.0±1.4	23.0±2.6	8.7±2.0	5

\*\* Scintillation was high during these measurements.

is extremely sensitive to receiver misalignment. According to that data, over 35 per cent is lost in transmission reading by angular displacements as small as  $\pm 1$  mrad. Consequently, any flexing in the floor support of the receiver would cause the transmission reading to change when the person accomplishing the receiver alignment moved away from the receiver. This applies to positions 3 and 4.

2. The peak sensitivity position is not necessarily in the center of the circle superimposed in the optical viewfinder image.

3. Changing the near IR electronics drawer position can change the transmission reading by as much as 10 to 15 per cent.

4. Turning the visible light source off reduced the near IR transmission reading from over 40 per cent down to 10 per cent.
5. If the receiver is at one window and the transmitter assembly is aligned with the adjacent window, the transmission readings are substantially lower than would be predicted for the larger source apertures and vary substantially less as a function of source aperture size. Representative data are shown in table III including an indication as to whether or not the central spot size should overlap the adjacent window.
6. Scintillation increases the spread in the data even for the largest aperture.

Table III. Adjacent Window Measurements

Source Aperture Diameter (inch)	Transmission Reading	Spot Size Overlap ?
0.1405	12.0	yes
.0810	12.2	yes
.0444	10.7	yes
.0256	9.1	marginal
.0141	8.6	no
0.0081	8.6	no

NOTE: The readings increased to 19.0 when the transmitter assembly was aligned to this window.

Discussion. The results of the weather tower tests do not demonstrate conclusively that the tower does or does not have an effect on transmission measurements made at windows one or five. However, the data do permit one general conclusion to be drawn; that the beam profile is not as predicted from theory (see Table I) but has a smaller central cone. The

justification for this conclusion is contained in the following paragraphs.

Consider the slopes of the data plotted in figure 5. Variable alignment would explain the crossover on the 19 August data while different amounts of scintillation would account for the difference in slopes with the lower scintillation yielding the shallower slope on 20 August. The latter point is confirmed by the fact that the spread between the maximum and minimum readings was also reduced for less scintillation. Since using a flashlight at night helped eliminate the possibility of misalignment, the remainder of this discussion will be concerned only with the 24 August and 22 September data (figure 6 and table II).

At night, scintillation was quite a bit less than during the day and precise alignment of the transmitter assembly was assured by using a flashlight located at the receiver at the Trebein site. Although the slopes are even flatter, they still exist; the first aperture showing marked fall-off is the 0.256 aperture. Also, the difference between maximum and minimum readings is as great during the maximum scintillation period at night as during the day even though the scintillation appeared to be less visually; i.e., although the image of the flashlight sometimes moved out of the .0081 in. aperture at night, during the day the whole scene "crawled", and the image of the window sometimes moved most of the way out of the .0256 in. aperture. Since the diameter of the uniformly irradiated central cone is 3.69m for the 0.256 in. aperture,

nighttime scintillation should not reduce the transmission reading unless the central cone is smaller than predicted or is not uniform. Since the diameter of the central cone is only 0.88m for the 0.0081 in. aperture and 1.85m for the 0.0141 in. aperture, the transmission reading should be reduced by scintillation and the spread from maximum to minimum should be increased because the receiver would more often be illuminated by the energy from outside the central cone. The reading is reduced, but the spread is not increased; in fact, the spread is reduced. This also is explicable if the central cone is smaller than predicted. Finally, consider table III. If the central cone were as large as predicted, whenever the transmitter is aligned with one window, the transmission reading should be the same at the adjacent window as long as the central cone covers both windows. This is not the case; and, in fact, the transmission reading is still 37 per cent lower even when the central cone should be 22m (0.141 in. aperture).

The above comments are applicable to the data from each window considered by itself. When the data from the windows are compared to each other, it is obvious that at night, window two consistently provided higher transmission readings than the other positions. This can be traced to ease of alignment; at the southernmost window (3) and on the stairs (4), the flexibility of the floor is such that when the individual aligning the receiver moves away from it, its boresight is shifted. Also, at the normal window (1), the receiver

mounts were such that it was very difficult to "tweak" the boresight to within  $\pm 0.5$  mrad to assure maximum transmission readings.

### Calibration Test

Results. The modified LOWTRAN program was run to plot transmission as a function of wavelength and dew point and visibility. Samples of the three spectral region runs using the rural aerosol model are shown in figures 7 through 11. These plots were used in conjunction with the manufacturer's spectral calibration data to select the wavelengths to be used for the calibration tests. The tests were not run until the night of 24 September because, at first, gaseous nitrogen was not available and then the weather was too hazy; recall, the tests must be accomplished when scattering is not the principle attenuation mechanism. Only the near IR was available the night of the test. The results of the measurements are included in table V along with the LOWTRAN predictions using the rural, urban, and maritime aerosol models. The meteorological conditions during the test are listed in table IV.

Table IV. Meteorological Conditions During Cal Test

Parameter	B620	Trebein	Model
Temperature ( $^{\circ}\text{C}$ )	18	15	16
Dew Point ( $^{\circ}\text{C}$ )	13	14	14
Visibility (stat. mi)	12 (base wx)	8.5	8.5, 10, 12
Pressure (millibars)		985	985

Table V. Spectral Transmission Data

NOMINAL WAVELENGTH ( $\mu\text{m}$ )	MEASURED TRANSMISSION	LOWTRAN VISIBILITY (KM)								
		RURAL MODEL			URBAN MODEL			MARITIME MODEL		
		13.7	19.3	16.1	13.7	19.3	16.1	13.7	19.3	16.1
1.69	$71.5 \pm 5.4$	54.8	62.9	58.9	46.2	55.1		17.0	27.4	
1.73	$64.0 \pm 6.2$	44.0	50.2	47.0	36.9	44.3	40.6	13.6	21.8	17.3
2.23	$67.7 \pm 6.2$	66.8	73.1	70.0	56.4	64.8	60.5	21.5	32.7	26.7
2.27	$66.2 \pm 6.0$	68.1	74.3	71.2	57.6	66.0	61.8	22.2	33.5	27.4
3.99	$64.4 \pm 6.2$	54.8	58.5	56.7	50.1	54.9	52.5	21.4	30.0	25.5
4.03	$60.7 \pm 3.7$	50.8	51.2	52.5	46.5	50.9	48.7	20.0	28.0	23.8
4.05	$56.0 \pm 5.2$	47.4	50.5	49.0	43.4	47.5	45.5	18.8	26.2	22.3
4.62	$19.5 \pm 2.8$	26.0	27.7	26.9	24.2	26.3	25.2	11.6	15.6	13.5
4.67	$26.2 \pm 2.8$	30.5	32.4	31.4	28.3	30.8	29.6	13.7	18.4	15.9

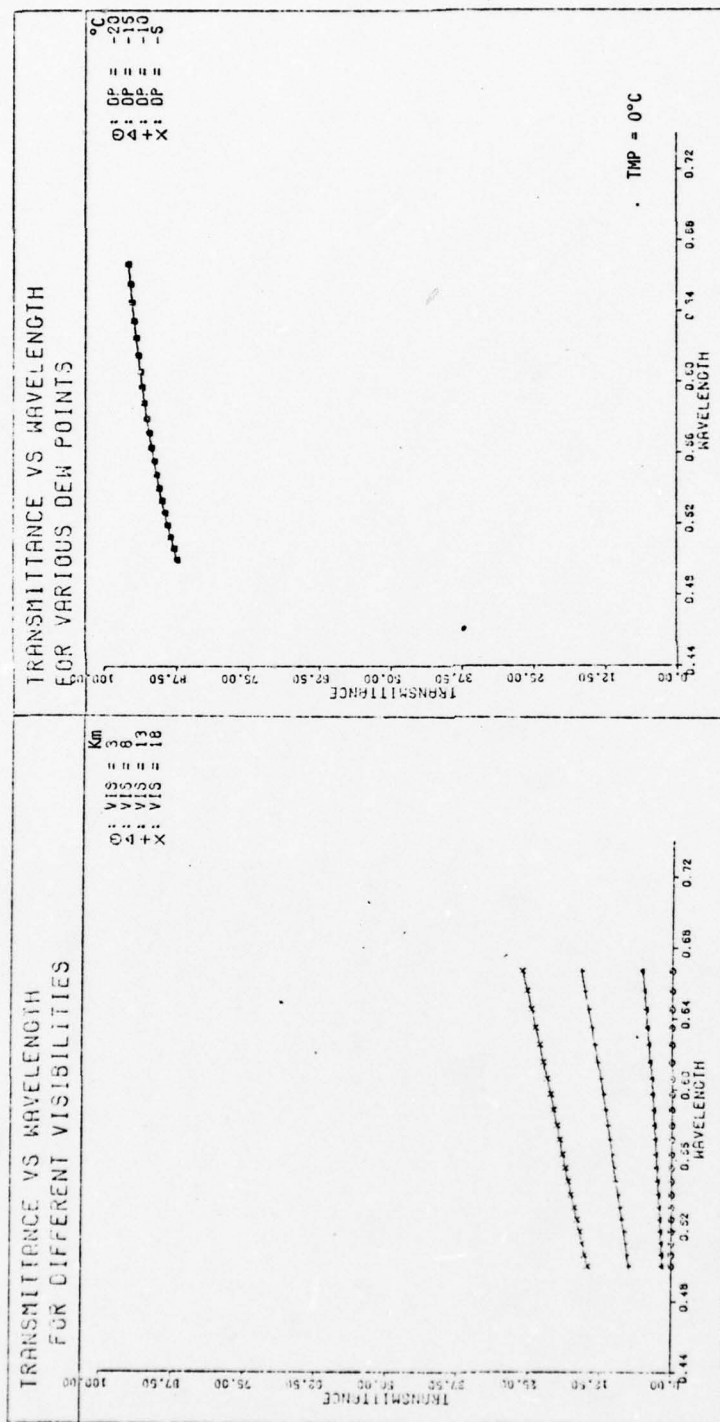


Fig. 7. Visible Spectral Transmission for Several Visibilities and Water Vapor Contents





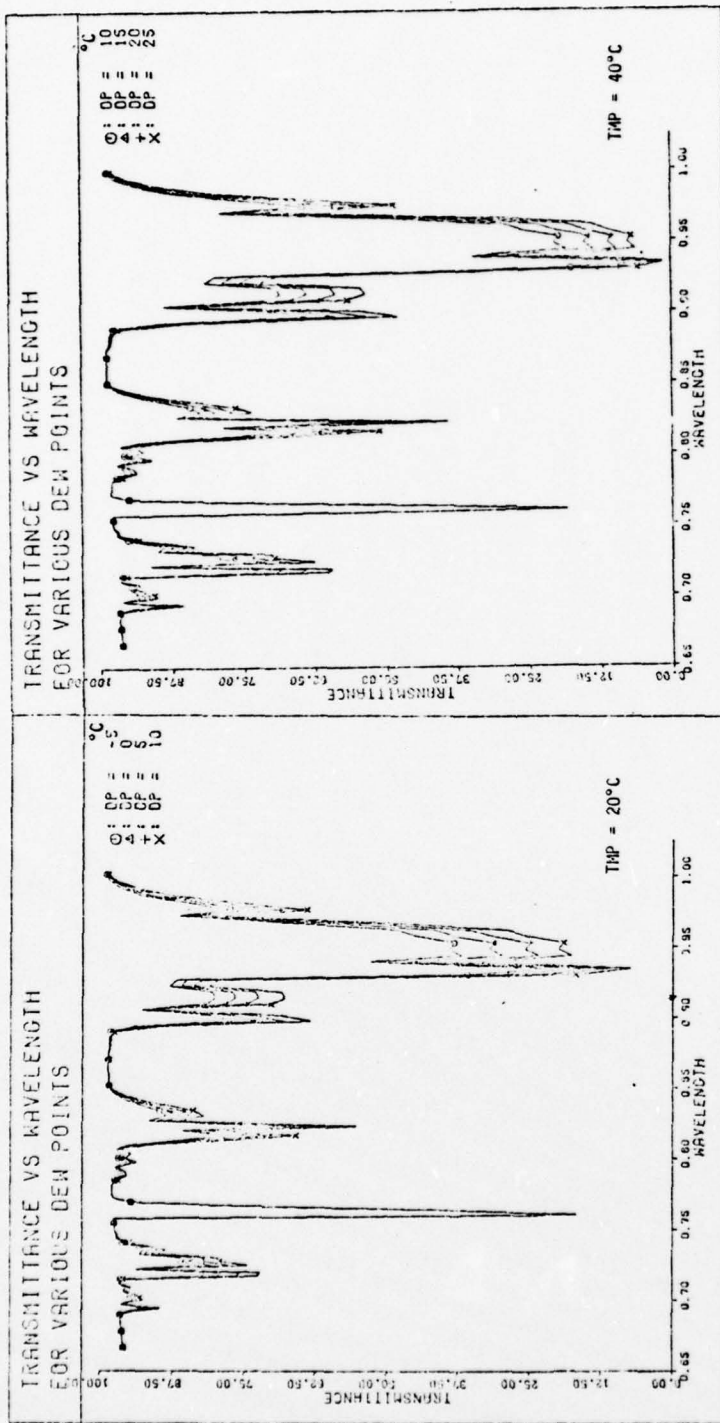


Fig. 8. Continued

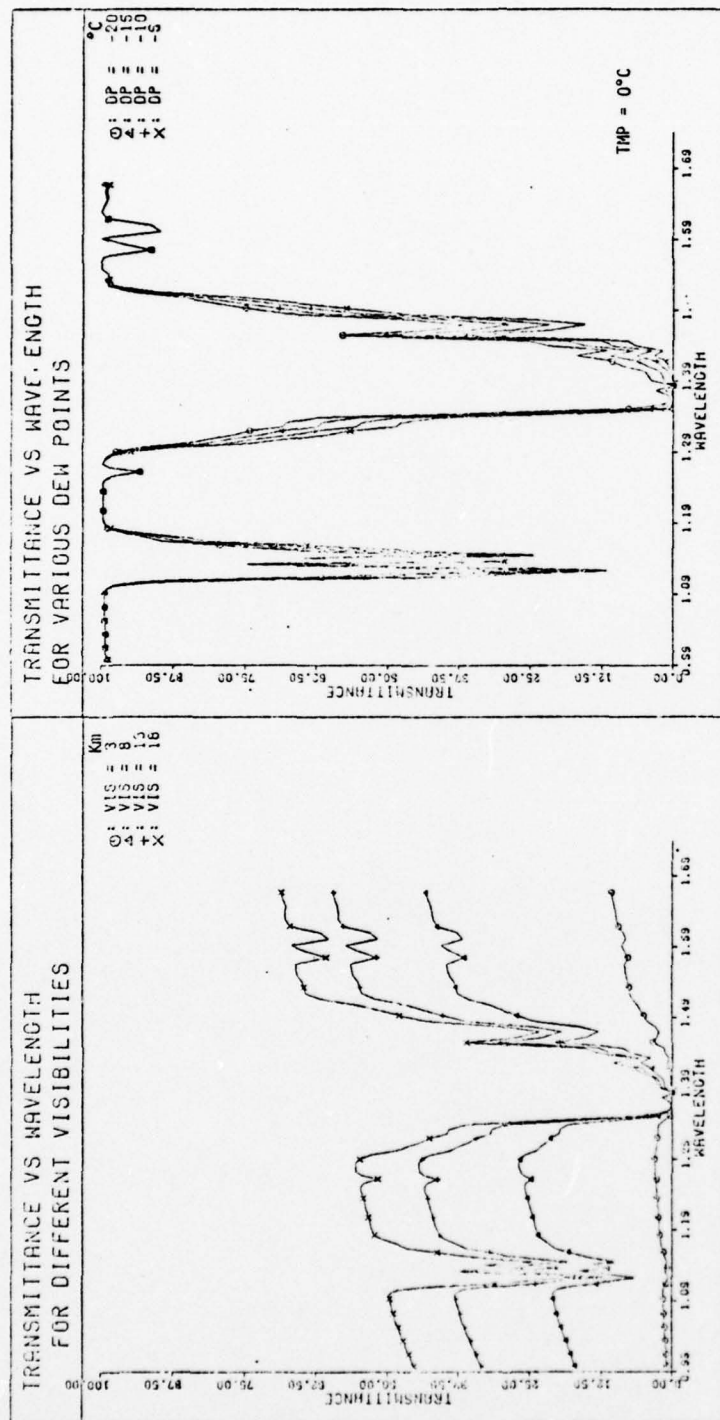


Fig. 9. Middle IR Spectral Transmittance for Several Visibilities and Water Vapor Contents

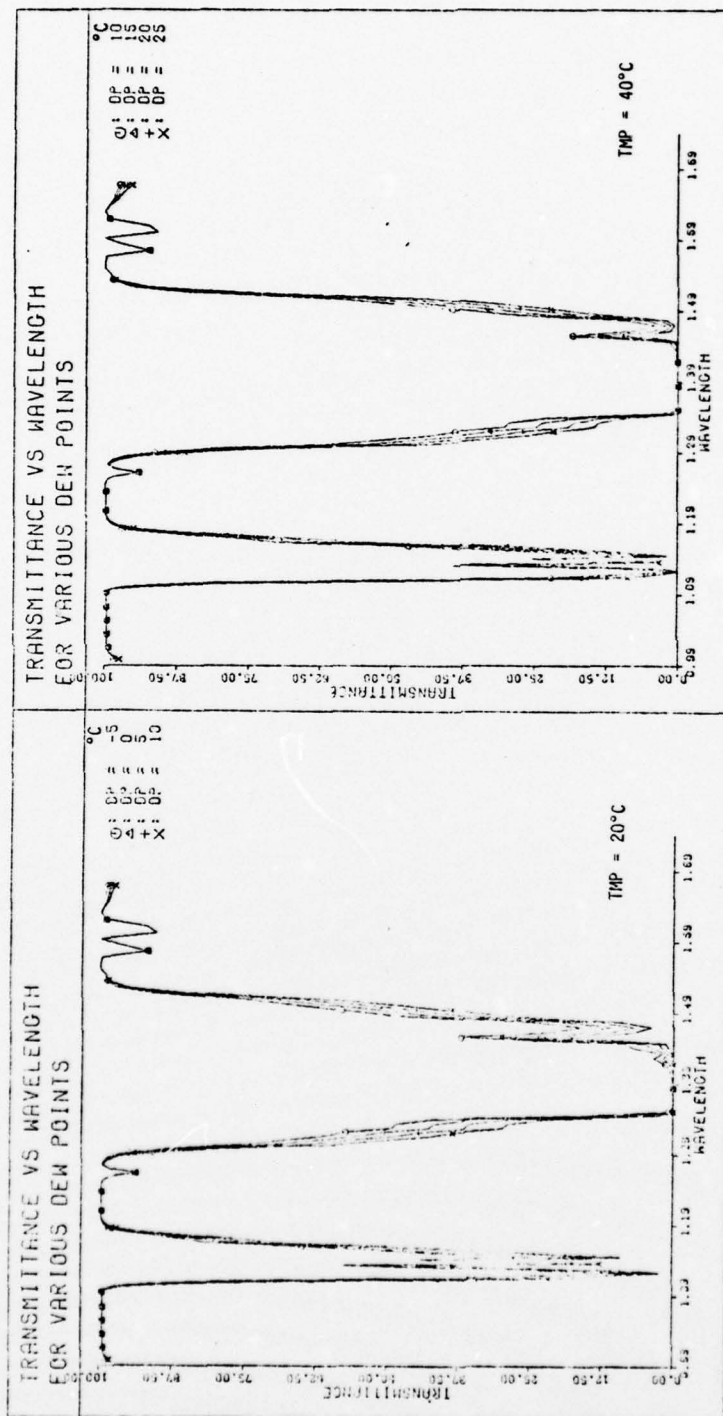


Fig 9. Continued

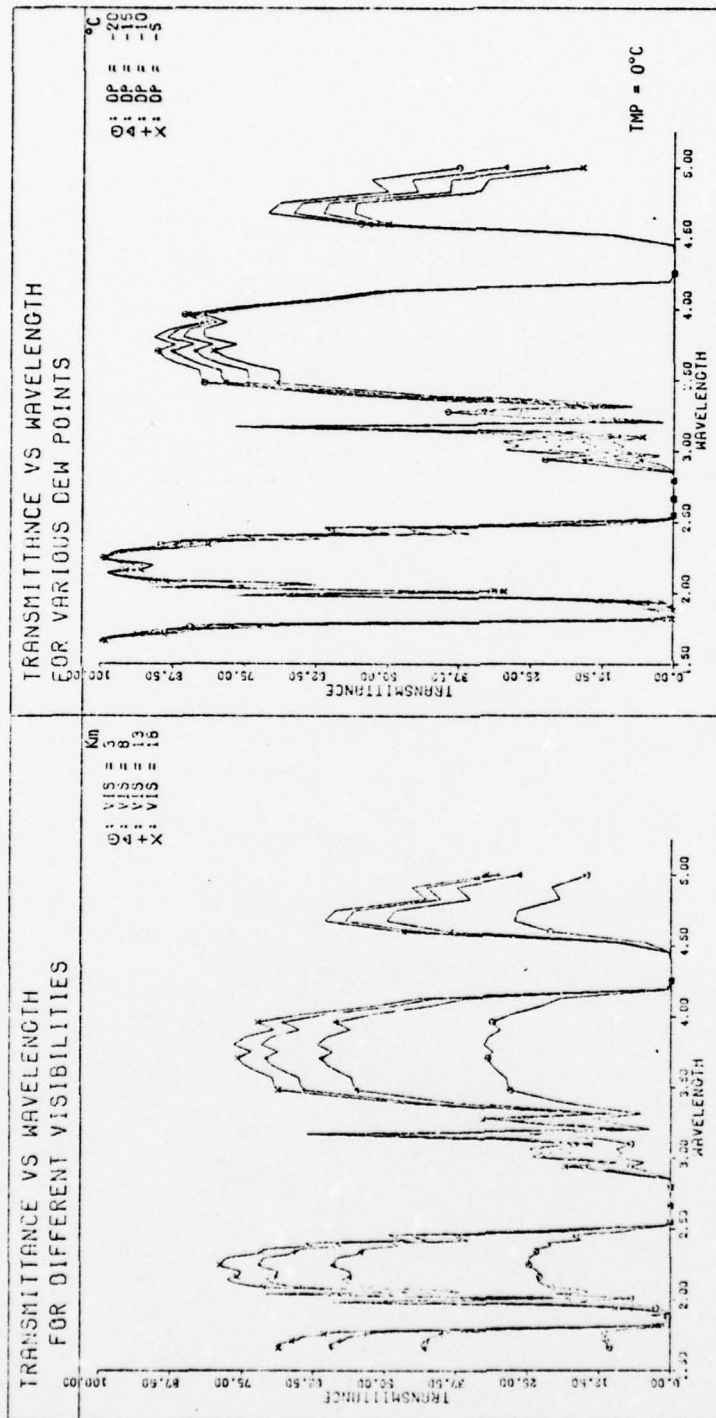


Fig. 10. Middle IR Spectral Transmission for Several Visibilities and Water Vapor Contents

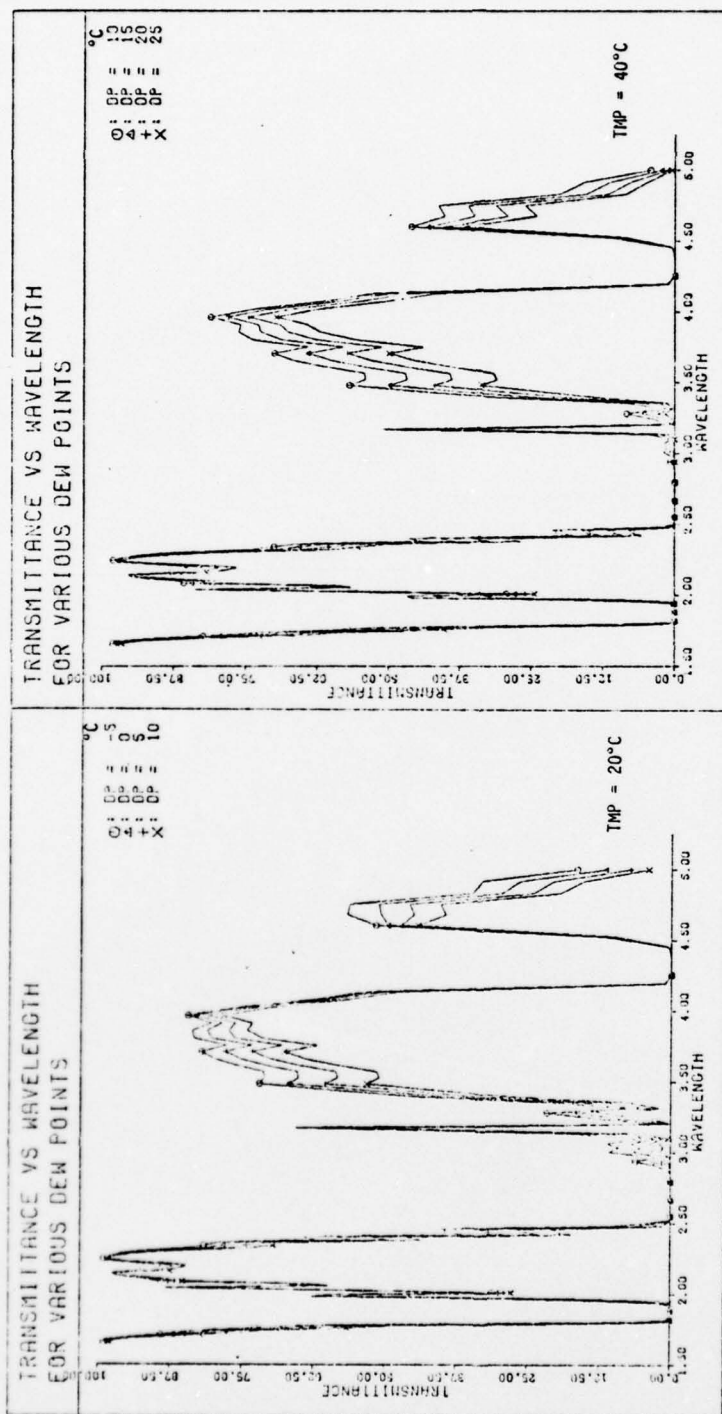


Fig. 10. Continued



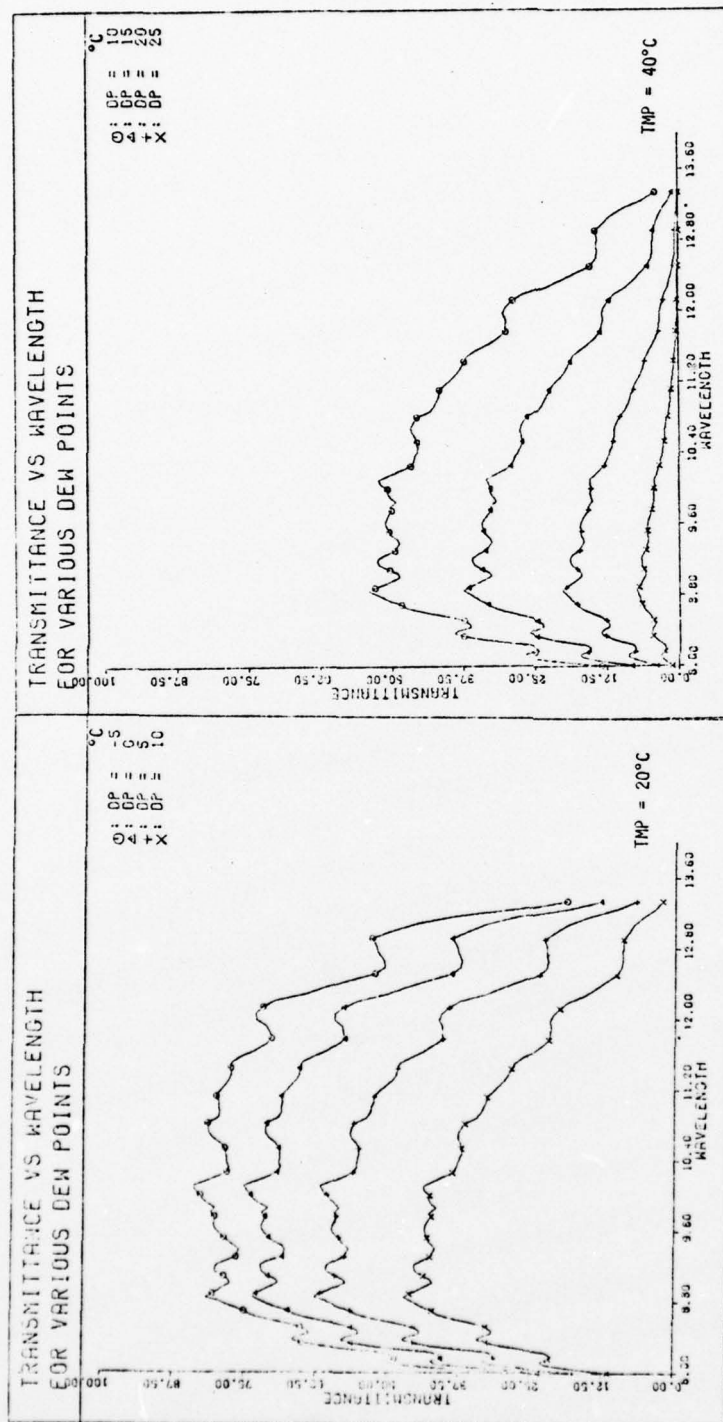


Fig. 11. Continued

After the *in situ* tests were completed, the near IR receiver and the electronics unit were brought to building 620. The dust cover was removed from the transmitter assembly, and the receiver was installed on an adjustable mount looking directly into the transmitter assembly. The calibration procedure of Appendix B was followed. Precision control of azimuth and elevation pointing angles was not possible; consequently, a great deal of time was required for each alignment, and the final alignment was still questionable. The temperature of the IR blackbody is not monitored by the control electronics; it did not look as deep red as during the *in situ* tests. The highest transmission reading for the CAL aperture, with the 10X attenuator in place, was 7.8 per cent. Moving the electronics drawer never caused the reading to exceed 20 per cent.

Discussion. With one exception ( $1.73\mu\text{m}$ ) the measured transmission values in table V are within 0.1 of the predicted values using the base weather visibility and the rural aerosol model in LOWTRAN III B; the lower  $1\sigma$  limit for that one wavelength interval is also within 0.1. Consequently, the calibration check in building 620 should have confirmed that no recalibration was required; this was not the case. Unfortunately, the adjustable mount was too difficult to use and an accurate alignment could not be proven. In addition, the variable transmission reading as a function of electronics drawer position caused much uncertainty in the procedure. Insufficient time remained to procure another mount and to

GEP/PH/77-14

repeat the experiment to demonstrate the efficacy of the *in situ* calibration check. The drawer position problem was subsequently traced to a faulty ground.

## V. Observations and Recommendations

### Observations

Using the Transmissometer. Because the transmitter beam central cone is not as large as expected, both the transmitter assembly and the receivers should be aligned prior to each test. Unfortunately, this will restrict test operations to days in which the visibility is five miles or greater. If the present transmitter mount proves to be sufficiently stable so that the realignment is not required, test days will still be restricted to those on which the transmission is greater than three per cent. This is because over half of the visible and almost half of the near IR channels have such low filter factors that the indicated transmission will be less than one per cent and the receiver will lose synch.

Also, scintillation appears to have a strong effect on the measurements. The frequency and amplitude of its effects are such that single point, instantaneous sampling could lead to an incorrect value.

Calibration. Although the current through the visible source is monitored and is constant, the radiation output will still change as the source ages. This leads to the need to recalibrate all three receivers, not just the visible receiver.

The temperature, dew point and visibility values at building 620, the Trebein site and Patterson field differ enough that more samples should be used, and the LOWTRAN calculation should be accomplished by steps between the sampling points.

Recommendations

1. Use receiver mounts with precision azimuth and elevation controls similar to those for small astronomical telescopes.
2. Use a rotary table with the same kind of mounts for calibration.
3. Permanently mount and boresight a high power telescope on top of the transmitter assembly. This will permit alignment without removing the IR source and beam splitter.
4. After three is accomplished, conduct a beam uniformity test and repeat the tower test.
5. Monitor the IR source temperature.
6. Provide an external synch for the receiver electronics.
7. Monitor temperature, dew point and visibility at all three meteorological instrumentation positions and, when using LOWTRAN, calculate the path transmission incrementally.
8. Determine the temperature/dew point variance along the path to determine if additional weather towers are required.
9. Verify the manufacturer's filter wheel spectral calibration and spectral resolution.
10. Conduct *in situ* calibration tests every time the visibility is greater than 15 km; use the data to select the most appropriate aerosol model; rural, urban or none; to use for the calibration graphs in Appendix B.

BIBLIOGRAPHY

1. Advisory Group for Aerospace Research & Development (AGARD). Optical Propagation in the Atmosphere. AGARD Conference Proceedings No. 183. AGARD, 1976.
2. AFAL-TR-76-214. Volume II. Appendix A. Atmospheric Effects at Optical Wavelengths. Air Force Avionics Laboratory, Wright-Patterson AFB, January, 1977.
3. AFAL-TR-76-217. Thermal Imaging System's Relative Performance, 3-5  $\mu\text{m}$  vs 8-12  $\mu\text{m}$ . Air Force Avionics Laboratory, Wright-Patterson AFB, January 1977.
4. Altshuler, T.L. A Procedure for Calculation of Atmospheric Transmission of Infrared. Report R57ELC 15. Ithaca, NY: General Electric Co. May 1, 1957.
5. Benford, F. "The Projection of Light", Journal of the Optical Society of America 35: 149-161. February, 1945.
6. Curcio, J.A. et al. Atmospheric Scattering in the Visible and Infrared, NRL Report 5567. Naval Research Laboratory, Washington, D.C., January, 1961.
7. Fenn, R.W. Chief, Atmospheric Optics Branch, Optical Physics Division, Air Force Geophysics Laboratory (personal correspondence). Hanscom AFB, MA, July 18, 1977.
8. Howard, J.N. and Garing, J.S. Transmission of the Atmosphere in the Infrared - A Review, AFCRL-62-814. Air Force Cambridge Research Laboratory, L G Hanscom Field, MA, July, 1962.
9. Hudson, R.A. Infrared System Engineering. Wiley, New York, NY, 1969.
10. Klein, M.V. Optics. Wiley, New York, NY, 1970.
11. Lloyd, J.M. Thermal Imaging Systems. New York: Plenum Press, 1975.
12. McCartney, E.J. Optics of the Atmosphere, Scattering by Molecules and Particles. Wiley, New York, NY, 1976.
13. McClatchey, P.A. et al. Optical Properties of the Atmosphere, AFCRL-TR-71-0279. Air Force Cambridge Research Laboratory, Hanscom AFB, MA, May 10, 1971.
14. Middleton, W.E. "The Effect of the Angular Aperture of a Telephotometer on the Telephotometry of Collimated and Non-collimated Beams", Journal of the Optical Society of America 39: 577-581. July, 1949.

15. Middleton, W.E. Vision Through the Atmosphere. University of Toronto Press, Toronto, Canada, 1952.
16. Roberts, R.E. Staff member, Institute for Defense Analyses (personal communication). Wright-Patterson AFB, OH, July 12, 1977.
17. Selby, J.E.A. et al. Atmospheric Transmittance from 0.25 to 28.5  $\mu$ m: Computer Code LOWTRAN 2, AFCRL-72-0745. Air Force Cambridge Research Laboratory, Hanscom AFB, MA, 1972.
18. Selby, J.E.A. et al. Atmospheric Transmittance from 0.25 to 28.5  $\mu$ m: Computer Code LOWTRAN 3, AFCRL-TR-75-0255. Air Force Cambridge Research Laboratory, Hanscom AFB, MA, 1975.
19. Selby, J.E.A. et al. Atmospheric Transmittance from 0.25 to 28.5  $\mu$ m: Supplement LOWTRAN 3B, AFGL-TR-76-0258. Air Force Geophysics Laboratory, Hanscom AFB, MA, 1976.
20. Stewart, H.S. and Curcio, J.A. "The Influence of Field of View on Measurements of Atmospheric Transmission, Journal of the Optical Society of America 42: 801-805. November, 1952.
21. Sundberg, E.E. Models for Predicting Electro-Optical Sensor Performance in Weather, AFIT Thesis GEP/PH/76-10. Air Force Institute of Technology, December, 1976.
22. The technical Cooperation Program (TTCP). Report of Action Group JAG-1. State of the Art of Airborne Forward Looking Infrared Technology (Vol I). TTCP, 1976.
23. Walsh, J.L. editor. Performance Modeling of Thermal Imaging Systems (draft). Washington, D.C.: Naval Material Command, 1977.
24. White, J.R. "Infrared Measurement Errors Caused by Spatial Response Nonuniformity". Unpublished tech note, Pacific Missile Test Center, Point Mugu, CA, undated.
25. Wolfe, W.L., editor. Handbook of Military Infrared Technology. Office of Naval Research, Washington, D.C., 1965.

Appendix A

Source Listing: Modified LOWTRAN IIIB

```

PROGRAM LT3HM (INPUT,OUTPUT,TAPE72,TAPE82,TAPE6=OUTPUT)
DIMENSION HZ1(34),HZ2(6),EH(10)
DIMENSION TR(67),FW(67),FO(67),HZ(2),TX(10),W(10)
DIMENSION C1(2580),C2(1575),C3(540),C4(133),C5(15),C6(102)
DIMENSION VX(45),C7(45),C7A(45)
F(A)=EXP(18.9766-14.9595*A-2.43882*A*A)*A
DATA H7(1)/5H23 KM/,H7(2)/5H 5 KM/
TXV=0
READ (82,401) (HZ1(I),I=1,34)
READ (82,401) (HZ2(I),I=1,5)
H72(6) = HZ1(6)
READ(82,431) (VX(I),C7(I),C7A(I),I=1,44)
READ (82,403) (TR(I),FW(I),FO(I),I=1,57)
READ (82,404) (C1(I),I=1,2580)
READ (82,404) (C2(I),I=1,1575)
READ (82,404) (C3(I),I=1,540)
READ (82,405) (C4(I),I=1,133)
READ (82,404) (C5(I),I=1,15)
READ (82,405) (C6(I),I=1,102)
JCNT=C
REWIND 72
2 CONTINUE
RCTR=0.0
PRINT*,"ENTER,IHAZE,JP,JSPEC,JTTY (+I3) "
READ*,IHAZE,JP,JSPEC,JTTY
PRINT 400,IHAZE,JP,JSPEC,JTTY
IF(JP.LE.2.AND.JSPEC.EQ.1)GO TO 903
IF(JP.GT.2.AND.JSPEC.EQ.2)GO TO 903
IF(JTTY.EQ.1.AND.IHAZE.EQ.7)IHAZE=1
IF(IHAZE.NE.7) GO TO 250
READ 431,(VX(I),C7(I),C7A(I),I=1,44)
PRINT 431,(VX(I),C7(I),C7A(I),I=1,44)
IHAZE = 1
250 CONTINUE
IF(JSPEC.NE.2)GO TO 107

```

```

IF (IXY.NE.3) GO TO 107
RANGE=RANGE+1.0
RCTR=RCTR+1.0
GO TO 105
107 CONTINUE
IF (IXY.GT.3) GO TO 541
IF (JITY.EQ.0) GO TO 251
PRINT*, "ENTER H1,P,IMP,DP,RH,WH,VIS,RANGE(KM,MB,C,C,%,GM M-3,KM,KM000520
1)"
251 READ*, H1,P,IMP,DP,PH,WH,VIS,RANGE
PRINT 430,H1,P,IMP,DP,RH,WH,VIS,RANGE
7=H1
J=FIX(Z+1.0E-6)+1.
IF (Z.GF.25.0) J=(Z-25.0)/5.0+26.
IF (Z.GF.50.0) J=(Z-50.0)/20.0+31.
IF (Z.GF.70.0) J=(Z-70.0)/30.0+32.
IF (J.GT.33) J=33
FAC=Z-FLOAT(J-1)
IF (J.LT.26) GO TO 500
FAC=(Z-5.0*FLOAT(J-26)-25.)/5.
IF (J.GF.31) FAC=(Z-50.0)/20.0
IF (J.GF.32) FAC=(Z-70.0)/30.0
IF (FAC.GT.1.0) FAC=1.0
500 L=J+1
IF (Z.GF.5.0) GO TO 520
AHZ2=H72(J)*(H72(L)/H72(J))**FAC
520 AHZ2=H71(J)*(H71(L)/H71(J))**FAC
541 CONTINUE
IF (IXY.GT.2) GO TO 542
IF (JITY.EQ.0) GO TO 510
PRINT*, "ENTER,V1,V2,DV (CM-1)"
510 READ*, V1,V2,DV
PRINT 406,V1,V2,DV
542 PRINT 407,H1,RANGE
IF (VIS.GT.0.0) PRINT 417,VIS

```

```

IF(VIS.LT.2.0.AND.VIS.GT.0.0) PRINT 442
IF (IHAZE.EQ.0.) PRINT 426
IF(VIS.LF.0.0.AND.IHAZE.GT.0) PRINT 416,IHAZE,H7(IHAZE)
AVW=10000./V1
ALAM=10000./V2
PRINT 418, V1,V2,DV,ALAM,AVW
AVW=0.5E-4*(V1+V2)
AVW=AVW*AVW
CO=77.46+.459*AVW
CW=43.487-0.3473*AVW
48 CONTINUE
LAX1=1
LAX2=1
LAX3=1
TMP=TMP-20.0
NP=NP+.0
IF(JP.LE.2)GO TO 14
IF(JP.GT.3)GO TO 13
VIS=VIS-5.0
LAX1=1
LAX2=1
LAX3=7
IF(JSPFC.EQ.1)LAX3=4
GO TO 14
13 LAX1=3
LAX2=7
TF(JSPFC.EQ.1)LAX2=4
LAX3=1
14 CONTINUE
SUMR=0.0
SUMV=0.0
SUMW=0.0
DO 909 II=1,LAX1
TMP=TMP+20.0
IF(II.EQ.1)GO TO 15

```

```

000900
000810
000820
000830
000840
000850
000860
000870
000880
000890
000900
000910
000920
000930
000940
000950
000960
000970
000980
000990
001000
001010
001020
001030
001040
001050
001060
001070
001080
001090
001100
001110
001120
001130
001140

```

001150  
001160  
001170  
001180  
001190  
001200  
001210  
001220  
001230  
001240  
001250  
001260  
001270  
001280  
001290  
001300  
001310  
001320  
001330  
001340  
001350  
001360  
001370  
001380  
001390  
001400  
001410  
001420  
001430  
001440  
001450  
001460  
001470  
001480  
001490

```

NP=NP-25.0
IF(JSPFC.EQ.1)DP=DP+23.0
15 CONTINUE
DO 909 JJ=1,LAX2
DP=DP+.5.0
DO 909 KK=1,LAX3
IF(JP.F0.3)VIS=VIS+5.0
IF(IXY.EQ.1)GO TO 49
T=TMP+273.15
TT=273.15/T
IF(RH.LE.0.0)TT=273.15/(273.15+DP)
IF(WH.LE.0.0)WH=F(TT)
IF(JP.F0.4)WH=F(TT)
IF(RH.GT.0.0)WH=0.01*.2H*WH
PS=P/1013.0
TS=273.15/T
X=PS*TS
PT=PS*SQRT(TS)
D=0.1*WH
EH(1)=D*PT*.0.9
EH(2)=Y*PT*.0.75
EH(4)=0.8*PT*X
PPW=4.56E-5*D*273.15/TS
TS1 = (296.0/273.15)*TS
EH(5)= D*PPW*EXP(6.08*(TS1-1.0))+0.002*D*(PS-PPW)
EH(10)=D*(PPW+0.12*(PS-PPW))*EXP(4.56*(TS1-1.0))
FH(6)=X
HAZE=AHAZE
IF(Z.GF.5.0) GO TO 150
IF(IHAZE.EQ.2)HAZE=AHZ2
IF(VIS.LE.0.0) GO TO 150
HAZE=6.389*((AHZ2-AHAZE)/VIS+AHAZE/5.0 -AHZ2/23.0)
150 IF(HAZE.LT.0.0) HAZE=0.0
FH(7) = HAZE/AHAZE
WO=5.6F-05

```

001500  
001510  
001520  
001530  
001540  
001550  
001560  
001570  
001580  
001590  
001600  
001610  
001620  
001630  
001640  
001650  
001660  
001670  
001680  
001690  
001700  
001710  
001720  
001730  
001740  
001750  
001760  
001770  
001780  
001790  
001800  
001810  
001820  
001830  
001840

```

EH(8)=46.6667*W0
EH(3)=EH(8)*PT**0.4
EH(9)=1.0
REF= 1.0E-6*(CO*X*1013.0/273.15-PPA*CW)
105 DO 27 K=1,10
27 W(K)=RANGE*EH(K)
49 CONTINUE
I=1
L=1
JCNT=JCNT+1
IV1=V1/5.0
IV2=V2/5.+.99
IV1=5*IV1
IV2=5*IV2
IF (IV1.LT.350) IV1=350
IF (IV2.GT.5000) IV2=5000
IF (OV.LT.5.)OV=5.
IOV=OV
N=FLOAT(IV2-IV1)/OV+1
IF (II.FO.1.AND.JJ.EQ.1.AND.KK.EQ.1)WRITE(72)JSPEC,JP,N
IF (JSPFC.EQ.1.OR.(JJ.EQ.1.AND.KK.EQ.1))WRITE(72)TMP,OP,VIS
IV=IV1-IOV
ICOUNT=0
SUMA=0.0
C**+ BEGINNING OF TRANSMITTANCE CALCULATIONS
50 IV=IV+IOV
IF (JP.EQ.0)GO TO 51
IF (JP.EQ.2.OR.JSPEC.EQ.1)GO TO 51
GO TO 52
51 IF (ICOUNT.EQ.50) ICOUNT=0
IF (ICOUNT.EQ.0)PRINT 422
52 DO 53 K=1,10
TX(K)=C.C
IF (K.LT.4) TX(K)=1.0
53 CONTINUE

```

001850  
001860  
001870  
001880  
001890  
001900  
001910  
001920  
001930  
001940  
001950  
001960  
001970  
001980  
001990  
002000  
002010  
002020  
002030  
002040  
002050  
002060  
002070  
002080  
002090  
002100  
002110  
002120  
002130  
002140  
002150  
002160  
002170  
002180  
002190

```

ICOUNT=ICOUNT+1
SUM=0.0
V=IV
I=(IV-350)/5+1
IF (IV.LT.670) GO TO 72
IF (IV.LE.3000) GO TO 61
C***** MOLECULAR SCATTERING
C6=9.807E-20*(V**4.0117)
TX(6)=C6*W(6)
SUM=SUM+TX(6)
IF (IV.LT.9200) GO TO 72
IF (IV.LT.13000) GO TO 69
C***** UV OZONE
IF (IV.LE.23400) GO TO 54
IF (IV.GE.27500) GO TO 55
GO TO 87
54 XX=200.0
XI=(V-13000.0)/XX+1.0
L1=1
L2=53
GO TO 66
55 XX=500.0
XI=(V-27500.0)/XX+57.0
L1=57
L2=102
56 DO 57 NN=L1,L2
XD=XI-FLOAT(NN)
IF (XD) 59,58,57
CONTINUE
58 TX(8)=W(8)*C8(NN)
GO TO 60
59 TX(8)=C8(NN)+XD*(C8(NN)-C8(NN-1))
TX(8)=W(8)*TX(8)
SUM=SUM+TX(8)
50 IF (IV.GT.14500) GO TO 87

```

```

50 TO 69
C***** WATER VAPOR CONTINUUM 10 MICRON REGION
51 IF (IV.GT.1350) GO TO 62
TX(5) = (4.18 + 5578.0 * EXP(-7.87E-3*V)) * W(5)
GO TO 66
62 IF (IV.LT.2350) GO TO 68
C***** WATER VAPOR CONTINUUM 4 MICRON REGION
XI = (V-2350.0) / 50.0 + 1.0
NH = XI + 1.001
XH = XI - FLOAT(NH)
TX(5) = C5(NH)
TX(5) = TX(5) * XH * (C5(NH) - C5(NH-1))
TX(5) = TX(5) * W(10)
SUM = SUM + TX(5)
65 IF (IV.LE.1350.OR.IV.GT.2740) GO TO 72
C***** NITROGEN CONTINUUM
58 IF (IV.LT.2080) GO TO 72
K4 = I-36
TX(4) = C4(K4) * W(4)
SUM = SUM + TX(4)
GO TO 72
C***** WATER VAPOUR
59 IF (IV.LT.12800.AND.IV.GE.9875) GO TO 70
IF (IV.LE.14520.AND.IV.GE.13400) GO TO 71
GO TO 76
70 I = I-13F
GO TO 72
71 I = I-25F
72 K1 = 1
IF (W(1).LT.1.0E-20) GO TO 76
WS1 = ALOG10(W(1)) + C1(I)
IF (WS1.LT.-2.3468) GO TO 76
IF (WS1.GT.3.5682) GO TO 75
IF (WS1.GT.2.0) K1 = 40
DO 73 K = K1, 67

```

```

002200
002210
002220
002230
002240
002250
002260
002270
002280
002290
002300
002310
002320
002330
002340
002350
002360
002370
002380
002390
002400
002410
002420
002430
002440
002450
002460
002470
002480
002490
002500
002510
002520
002530
002540

```

```

73 IF (WS1.LE.FW(K)) GO TO 74
74 CONTINUE
75 TX(1)=TR(K)+(TR(K-1)-TR(K))*(FW(K)-WS1)/(FW(K)-FW(K-1))
76 GO TO 76
77 TX(1)=0.0
78 CONTINUE
79 C***** UNIFORMLY MIXED GASES
80 IF (IV.LT.8060.AND.IV.GT.500) GO TO 77
81 IF (IV.LT.13190.AND.IV.GT.12970) GO TO 78
82 GO TO 83
83 J=I-30
84 GO TO 79
85 J=(IV-12950)/5+1516
86 IF (W(2).LT.1.0E-20) GOTO 83
87 K1=1
88 WS2=ALOG10(W(2))+C2(J)
89 IF (WS2.LT.-2.3468) GO TO 83
90 IF (WS2.GT.3.5682) GO TO 82
91 IF (WS2.GT.2.0) K1=40
92 DO 30 K=K1,67
93 IF (WS?.LE.FW(K)) GO TO 81
94 CONTINUE
95 TX(2)=TR(K)+(TR(K-1)-TR(K))*(FW(K)-WS2)/(FW(K)-FW(K-1))
96 GO TO 83
97 TX(2)=0.0
98 CONTINUE
99 C***** OZONE
100 C*****CALCULATED FOR Z.LT.2 WITH W0.E0.5.5E-05
101 IF (IV.LT.575.0R.IV.GT.3270) GO TO 87
102 L=I-45
103 K1=1
104 IF (W(2).LT.1.0E-20) GO TO 87
105 WS3=ALOG10(W(3))+C3(L)
106 IF (WS3.LT.-1.6778) GO TO 87
107 IF (WS3.GT.3.9345) GO TO 86

```

```

      IF (WSZ.GT.1.5) K1=36
      DO 34 K=K1,67
      IF (WSZ.LE.FO(K)) GO TO 85
      CONTINUE
34    TX(3)=TR(K)-(TR(K)-TR(K-1))*(FO(K)-4S3)/(FO(K)-FO(K-1))
35    GO TO 87
      TX(3)=0.0
36    CONTINUE
37    ***** AEROSOL EXTINCTION
      ALAM=1.0E+4/V
      XX=0.0
      YY=0.0
38    ***** IF TEMPORARY FOG CORRECTION FOR VIS BELOW 2 KM.
      IF (IHA7E.EQ.0) GO TO 90
      IF (VIS.GT.0.0.AND.VIS.LT.2.0) XX = 3.91/VIS
      IF (XX.GT.0.0) GO TO 90
      DO 88 NN=1,44
      XD=ALAM-VX(NN)
      IF (XD) 89,88,88
39    CONTINUE
      XX=(C7(NN)-C7(NN-1))*XD/(VX(NN)-VX(NN-1))+C7(NN)
      YY=(C7A(NN)-C7A(NN-1))*XD/(VX(NN)-VX(NN-1))+C7A(NN)
90    TX(10)=YY*W(7)
      TX(7)=XX*W(7)
      SUM=SUM+TX(7)
      TX(9)=SUM
      DO 94 K=4,10
      IF (TX(K).EQ.0.0) GO TO 92
      IF (TX(K).LE.0.1) GO TO 91
      IF (TX(K).GT.20.) GO TO 93
      TX(K)=EXP(-TX(K))
      GO TO 94
31    TX(K)=1.0-TX(K)+0.5*TX(K)+TX(K)
      GO TO 94
32    TX(K)=1.0

```

```

33      GO TO 94
34      TX(K)=0.
      CONTINUE
      SUMV=SUMV+TX(7)
      HOH=TX(1)*TX(5)
      IF(JP.EQ.2.AND.JTYY.EQ.1)WRITE(6,++3)HOH
      SUMW=SUMW+HOH
      TX(10)=1.0-TX(10)
      TX(9)=TX(1)*TX(2)+TX(3)*TX(9)
      IF(IV.GE.13000)TX(3)=TX(8)
      AR=1.0-TX(9)
      IF(IV.EQ.IV1.OR.IV.EQ.IV2)AR=0.5*AR
      SUMA=SUMA+AR*DV
      IF(JP.EQ.0.OR.JP.EQ.2)WRITE(6,423)IV,ALAM,TX(9),(TX(K),K=1,7),
1 TX(10),SUMA
      IF(JSPEC.EQ.1)WRITE(6,423)IV,ALAM,TX(9),(TX(K),K=1,7),TX(10),SUMA
      TN=TX(9)*100
      IF(JP.EQ.2)WRITE(72)ALAM,TN
      IF(JSPEC.EQ.1)WRITE(72)ALAM,TN
      IF(IV.GE.IV2)GO TO 95
      GO TO 90
95      AB = 1.0 - SUMA/ FLOAT(IV2-IV1)
      PRINT 424,IV1,IV2,SUMA,AR
      PRINT*,"TMP=",TMP," DP=",DP," VIS=",VIS," JP=",JP," JSPEC=",JSPEC
      PRINT*,"RANGE=",RANGE
      IF(JP.LT.2)GO TO 909
      PRINT*,"N=",N
      SUMW=SUMW/N
      SUMV=SUMV/N
      IF(SUMV.LE.0.0)PRINT*,"SUMR WON'T COMPUTE"
      SUMR=0.999
      IF(SUMV.GT.0.0)SUMR=AR/(SUMV*SUMW)
      PRINT 445,SUMW
      PRINT 446,SUMV
      PRINT 447,SUMR
003250
003260
003270
003280
003290
003300
003310
003320
003330
003340
003350
003360
003370
003380
003390
003400
003410
003420
003430
003440
003450
003460
003470
003480
003490
003500
003510
003520
003530
003540
003550
003560
003570
003580
003590

```

```

SUMV=100*SUMV
SUMW=100*SUMW
IF(JSPEC.EQ.1)GO TO 646
IF(JP.EQ.3)WRITE(72)VIS,SUMV
IF(JP.EQ.4)WRITE(72)DP,SUMW
636 CONTINUE
SUMR=0.0
SUMV=0.0
SUMW=0.0
309 CONTINUE
IF(JSPEC.NE.2)GO TO 106
IF(RANGE.GE.25.0.OR.A3.LE.0.0001)GO TO 106
IXY=3
GO TO 250
106 IF(JTYY.EQ.1)PRINT*,"ENTER IXY (I3) "
READ 400,IXY
IF(JSPFC.EQ.2)RANGE=RANGE-RCR
RCR=0.0
PRINT*,"JCNR= ",JCNR
PRINT*,"IXY= ",IXY
IF(IXY.EQ.0) GO TO 100
GO TO (96,2,107,97,100), IXY
96 IF(JTYY.EQ.3)GO TO 787
PRINT*,"ENTER V1,V2,DV (CM-1) "
787 CONTINUE
READ*, V1,V2,DV
AVW=10000./V1
ALAM=10000./V2
PRINT 418, V1,V2,DV,ALAM,AVW
IF(JP.LE.2)GO TO 48
97 IF(JP.NE.3)GO TO 98
VIS=VIS-30.0
IF(JSPEC.EQ.1)VIS=VIS+15.0
IF(IXY.EQ.1)GO TO 48
IF(IXY.EQ.4)GO TO 2
003600
003610
003620
003630
003640
003650
003660
003670
003680
003690
003700
003710
003720
003730
003740
003750
003760
003770
003780
003790
003800
003810
003820
003830
003840
003850
003860
003870
003880
003890
003900
003910
003920
003930
003940

```

```

98 IF(JP.NE.4)GO TO 2
   WH=0.0
   TMP=TMP-40.0
   DP=DP-50.0
   IF(JSPFC.EQ.1)DP=DP+5.0
   IF(IXY.EQ.1)GO TO 48
   IF(IXY.EQ.4)GO TO 2
100 STOP
400 FORMAT(10I3,F10.3)
401 FORMAT (8E10.3)
403 FORMAT (4(F6.3,2F7.4))
404 FORMAT (15F5.2)
405 FORMAT (8E9.2)
406 FORMAT (7F10.3)
407 FORMAT (/10X,28H HORIZONTAL PATH, ALTITUDE =,F7.3,12H KM, RANGE =004090
1,F7.3,3H KM)
416 FORMAT (/20X,12H HAZE MODEL ,I1,3H = ,A5,13H VISUAL RANGE)
417 FORMAT (/25X+HAZE MODEL =*,F5.1,* KM VISUAL RANGE AT SEA LFLVL*) 004110
418 FORMAT (/10X,21H FREQUENCY RANGE V1= ,F7.1,13H CM-1 TO V2= ,F7.1,1004130
14H CM-1 FOR DV =,F6.1,9H CM-1 (,F5.3,* - *,F6.3,* MICRONS )*) 004140
422 FORMAT (1H1,/10X,32H FREQ WAVELENGTH TOTAL H20,5X4HC02+,5X,6004150
14H070NE N2 CONT H2O CONT MOL SCAT AEROSOL AEROSOL INTEGRATED004160
2 /11X,14H CM-1 MICRONS,p(4X,5HTRANS),+X,20H ABS ABSORPTION ) 004170
423 FORMAT (10X,I6,10F9.4,F12.2) 004180
424 FORMAT(/* INTEGRATED ABSORPTION FROM*,I5,* TO*,I5,* CM-1 =*,F10.2,004190
1*, AVEPAGE TRANSMITTANCE=*,F7.5) 004200
426 FOPMAT (/20X,*AEROSOL SCATTERING NOT COMPUTED,IHA7F=0*) 004210
+30 FORMAT(10X," INPUT METEOROLOGICAL DATA"/10X,"Z=",F7.2,"KM, P=",F7.004220
12,*MB, T=*,F5.1,*C, DEW PT=*,F5.1,*C, RH=*,F5.1,*%, WH=*,E10.3,*GM004230
2 M-3, VIS RGE=*,F6.1,*KM, RGE=*,F10.3,*KM*) 004240
431 FORMAT (4(F6.2,2F7.5)) 004250
442 FORMAT(* FOG CONDITIONS MAY EXIST AT SEA LEVEL FOR THIS VISUAL PA004260
1NGE*,/* IF SO THEN ASSUME THE TRANSMITTANCE DUE TO FOG IS GIVEN 004270
2BY THE TRANSMITTANCE AT 0.55 MICRONS.*) 004280
443 FORMAT(2F7.3) 004290

```

004300  
004310  
004320  
004330  
004340  
004350

++4 FORMAT(F5.1,F7.3)  
+45 FORMAT(/9X,34H AVERAGE WATER VAPOR TRANSMISSION=,F7.5)  
+46 FORMAT(9X,34H AVERAGE AEROSOL TRANSMISSION =,F7.5)  
+47 FORMAT(9X,34H AVERAGE MOLECULAR TRANSMISSION =,F7.5)  
+48 FORMAT(9X,26H WATER VAPOR TRANSMISSION=,F7.5)  
END

Appendix B

Draft Calibration Handbook  
for  
Barnes Model 14-WP Transmissometer

As designed, the Barnes transmissometer is expected to require recalibration at three month intervals. Because of the difficulty of bringing the receiver and electronics to the transmitter assembly for calibration, it is desirable to use the transmission measurements themselves to determine when recalibration is required. This appendix discusses a technique for accomplishing this and then provides a step by step description of the calibration procedure.

#### Determine When Calibration is Required

The transmission measured by the Barnes Transmissometer can be separated into the transmissions of 3 different constituents of the atmosphere, the aerosols, the water vapor, and the remaining molecular absorption.

$$\tau_{\text{Total}} = \tau_{\text{Aerosol}} \times \tau_{\text{H}_2\text{O}} \times \tau_{\text{Mol}}$$

The aerosol transmission,  $\tau_{\text{Aerosol}}$ , is a function of visibility, VIS. The water vapor transmission,  $\tau_{\text{H}_2\text{O}}$ , is primarily a function of the dew point temperature,  $T_{\text{Dew}}$ , with a minor temperature dependence. The transmission by the other molecular absorbers can be considered a constant with a very weak temperature dependence. Given a knowledge of the visibility, dew point temperature, and the air temperature, it is possible to predict, within a few percent, the expected values of the transmission for each of the receivers of the Barnes Transmissometer. Figures B-1 through B-18 permit making these predictions. Figures B-1 through B-6 are for the visible receiver, B-7 through B-12 are for the near-IR

receiver and B-13 through B-18 are for the far-IR receiver. The following steps should be accomplished for each spectral band as indicated on the figures.

1. Using the visibility figure, find the predicted aerosol transmission,  $\tau_{\text{aerosol}}$ .

2. Using the dew point figure, select the temperature curve closest to the ambient temperature and find the predicted water vapor transmission,  $\tau_{\text{H}_2\text{O}}$ .

3. Using the curve labelled  $\tau_{\text{Mol}}$ , find the predicted molecular transmission.

4. The expected transmission for the appropriate wavelength is then the product of the three constituent transmissions.

$$\tau_{\text{Expected}} = \tau_{\text{Aerosol}} (\text{VIS}) \times \tau_{\text{H}_2\text{O}} (T_{\text{Dew}}) \times \tau_{\text{Mol}} (T)$$

5. If the measured transmissions are more than 0.1 lower than the expected transmissions for good visibilities (10 to 20 kilometers or better), the Barnes Transmissometer should be recalibrated.

#### Calibration Procedure

1. Remove the dust cover from the transmitter assembly
2. Mount the receiver to be calibrated onto a small rotary table and place the assembly on the telescope bed.

CAUTION. Do not bump the spider mirror.

3. Assure that the receiver optics are looking entirely into the telescope mirror. Use a sheet of white paper in front of the entrance aperture to confirm this.

4. Install the 10X attenuator in connector J2 on the mother board of the electronics unit for the receiver being calibrated.

5. Place the system in normal operation and use the JOG button to select the filter wheel position to the maximum response position as indicated in the manufacturer's calibration data book.

6. Select the 0.1405 inch aperture.

7. Rotate the receiver slowly in azimuth and elevation to produce the highest indication first on the ANALOG ALIGNMENT meter and then on the PERCENT TRANSMISSION digital readout indicator.

8. Lock the position settings on the Receiver Assembly.

9. Set the aperture wheel on the source to the next smaller setting and repeat Steps 4 through 8. Continue to repeat this procedure with smaller and smaller aperture settings until the one marked CAL is in position, then lock the rotary table.

10. On the Receiver, adjust the PHASE CONTROL knob to produce the maximum reading on the ANALOG ALIGNMENT Meter.

11. Observe the indication on the PERCENT TRANSMISSION display. If it is not 37.3, proceed to Step 12.

12. Unlatch the lower right panel in the receiver electronics unit and slide the chassis forward. Locate the calibration screwdriver adjustment at the upper right of the circuit board as seen from the component side. Rotate this

adjustment to produce a reading of 37.3 on the PERCENT TRANSMISSION digital display. Approach the 37.3 indication slowly by going up through lower indications and stopping as soon as 37.3 appears on the display.

At this point, the receiver is calibrated for the wavelength of maximum signal "Thru-put". Next, a printer is interfaced to the computer output connector. At each stopping position (wavelength), the BCD position is recorded along with the voltage displayed on the panel meter. The filter drive must be in AUTO mode. From this printout the factors are determined which will be used to normalize the data at each wavelength for a 37.3 reading with no path attenuation.

13. Recalibrate the other two receivers by using the same procedure.

14. The Atmospheric Transmissometer System is now recalibrated and can be placed back into normal use once the radiation source aperture wheel is returned to its initial position.

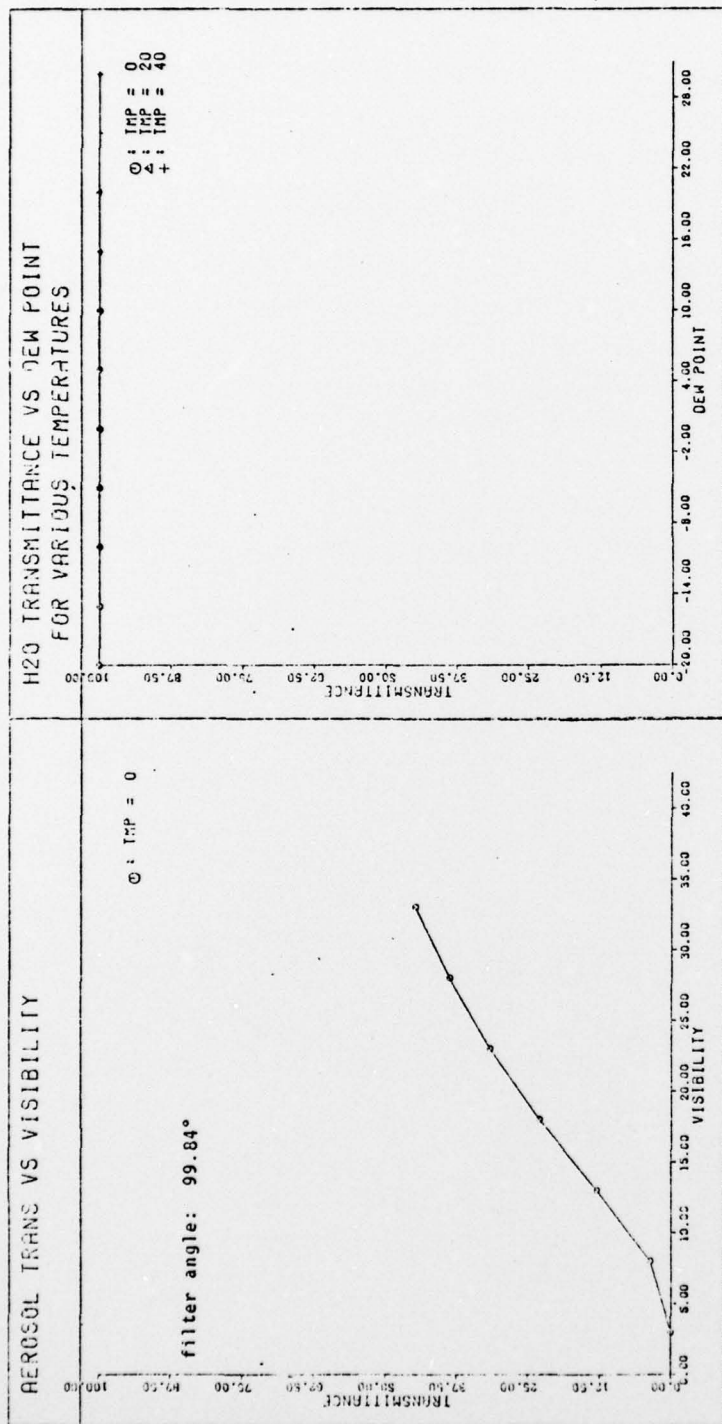


Fig. B1. 0.6 um Transmission as a Function of Visibility and Water Vapor Content

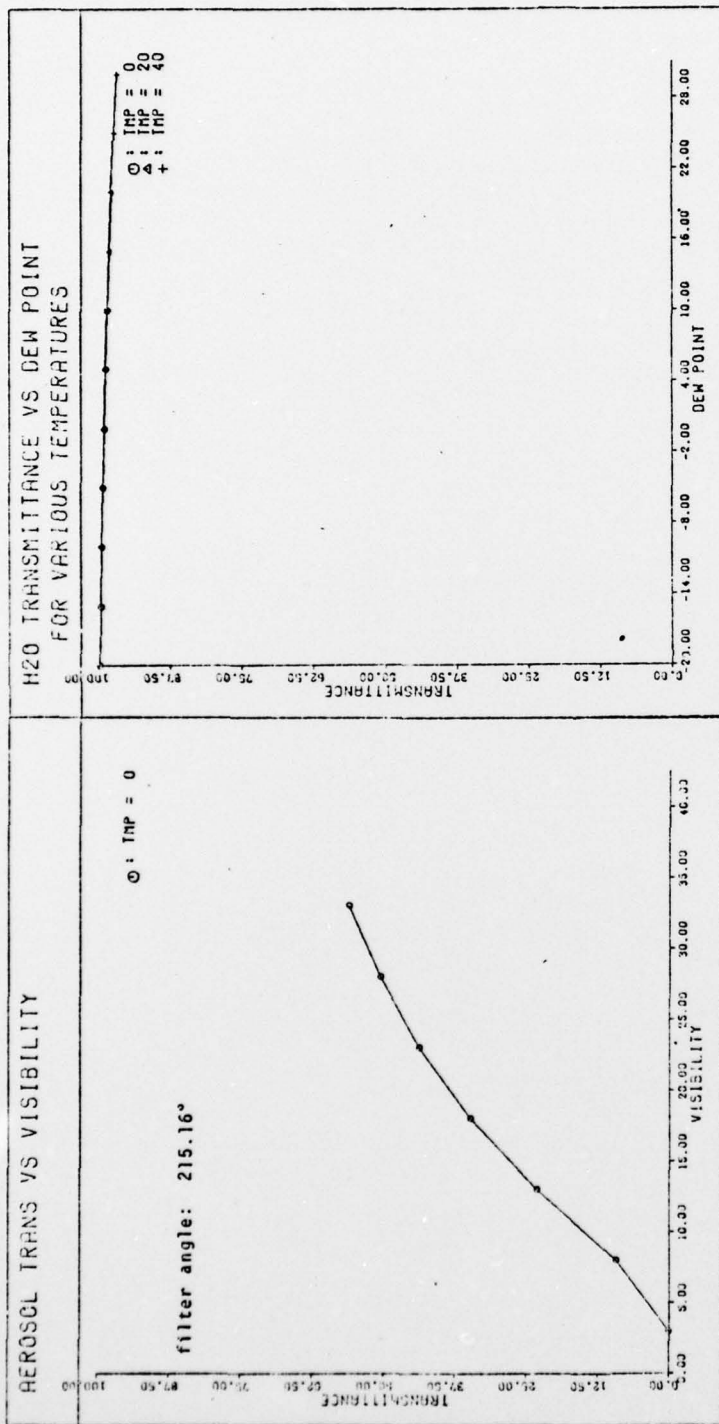


Fig. B2. 0.79 um Transmission as a Function of Visibility and Water Vapor Content

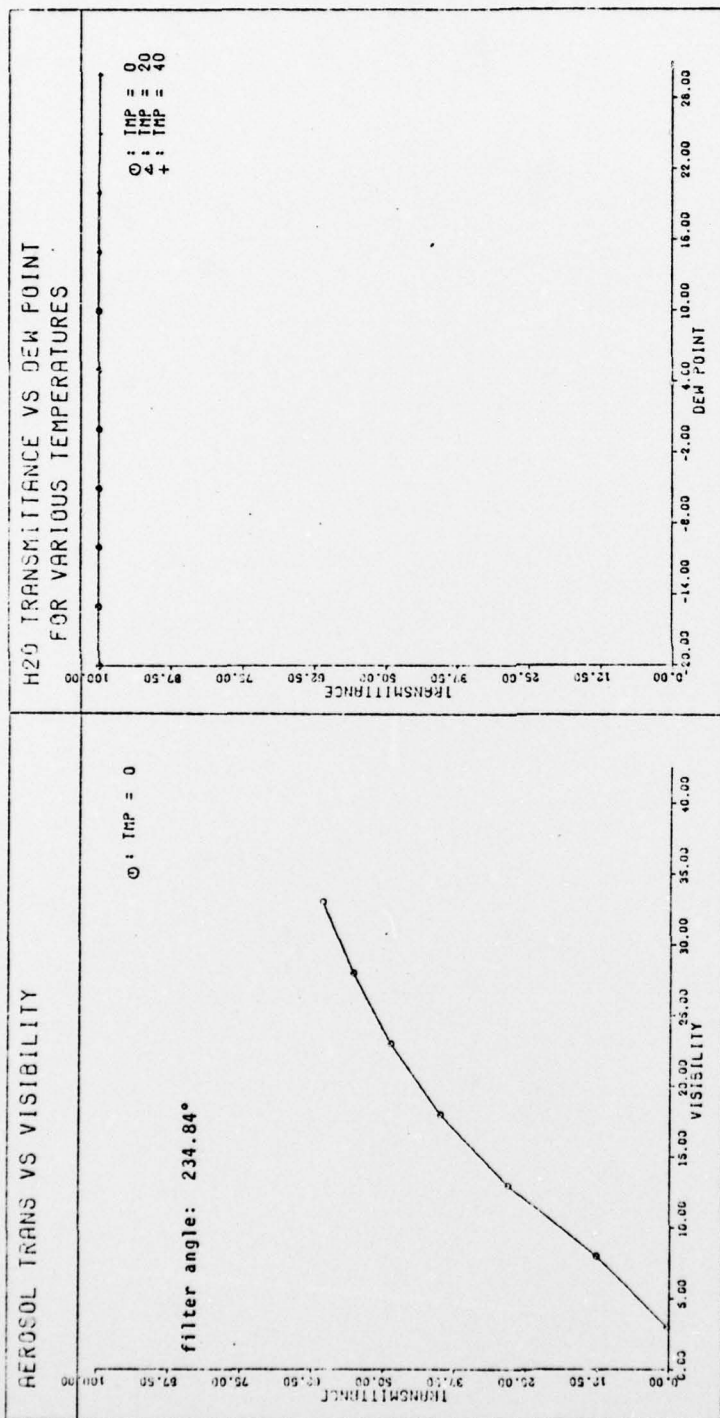


Fig. B3. 0.87  $\mu$ m Transmission as a Function of Visibility and Water Vapor Content

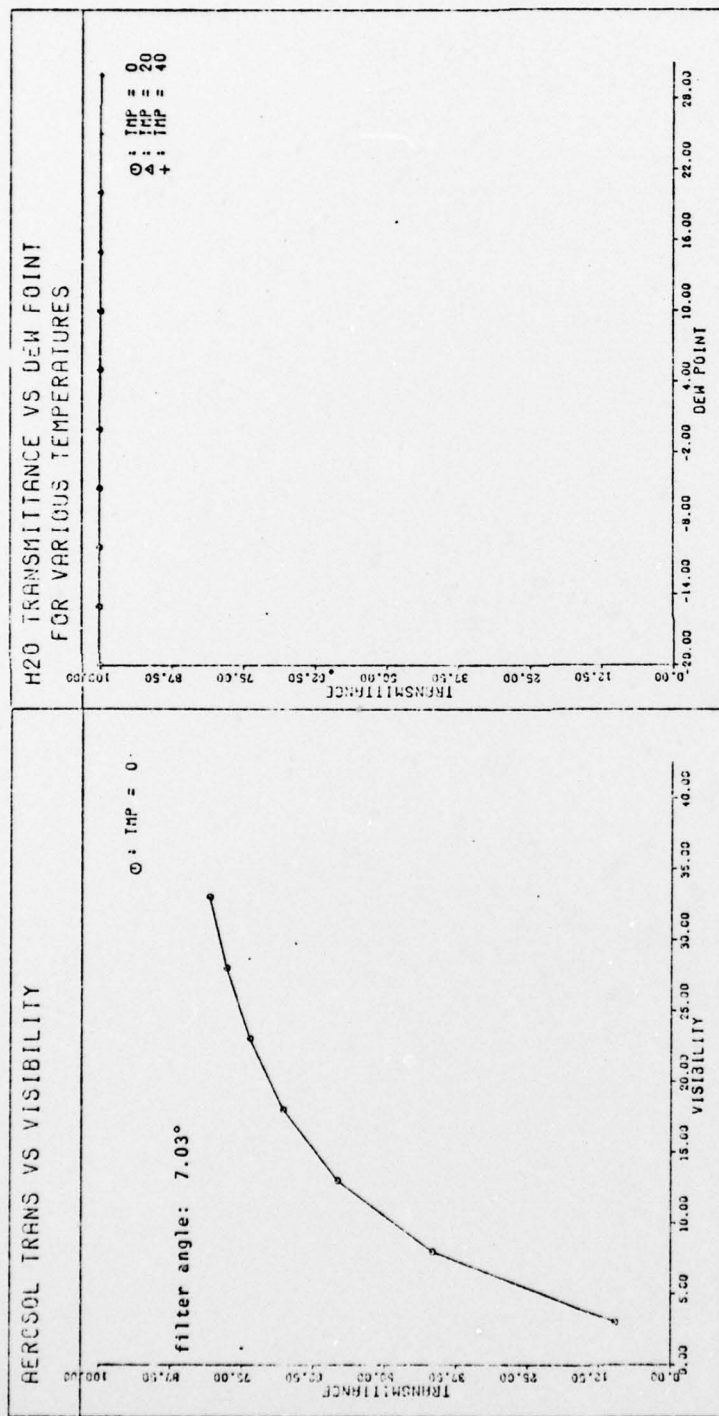


Fig. B4. 1.62  $\mu$ m Transmission as a Function of Visibility and Water Vapor Content

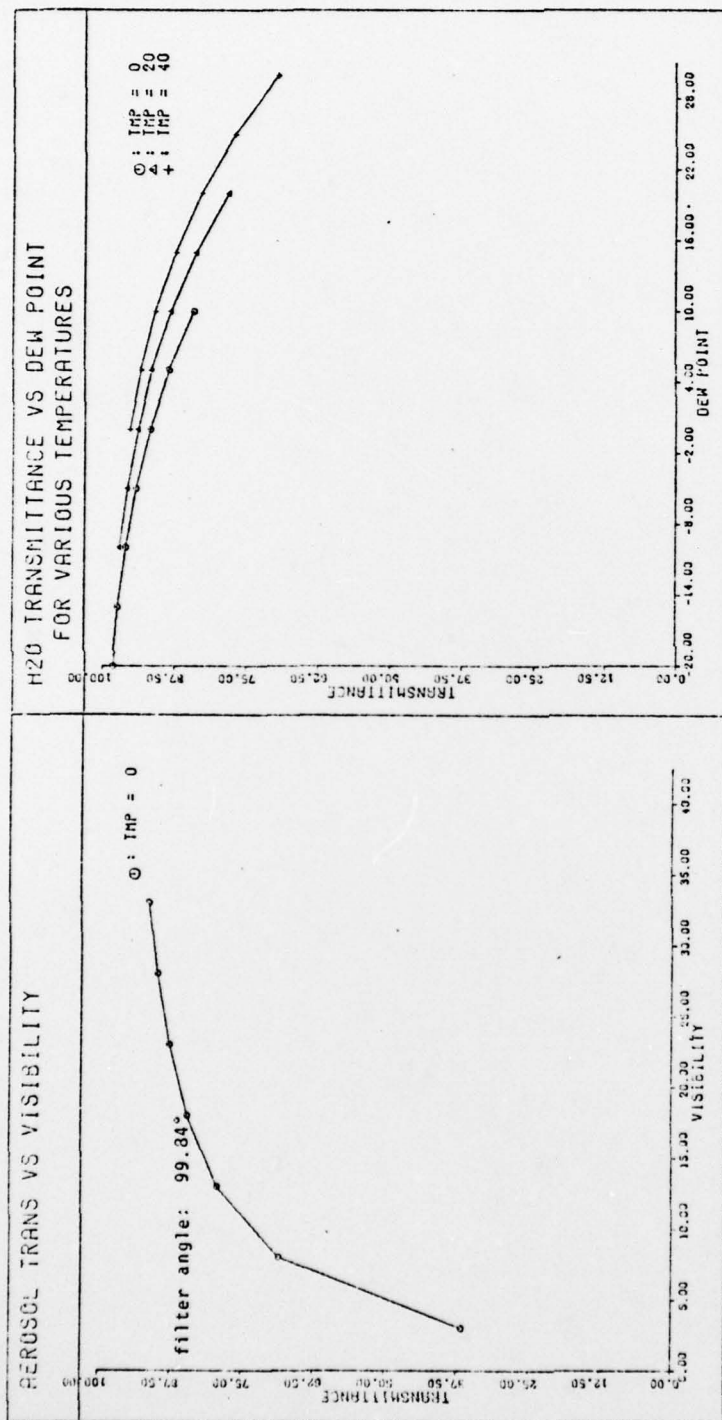


Fig. B5. 2.41  $\mu$ m Transmission as a Function of Visibility and Water Vapor Content

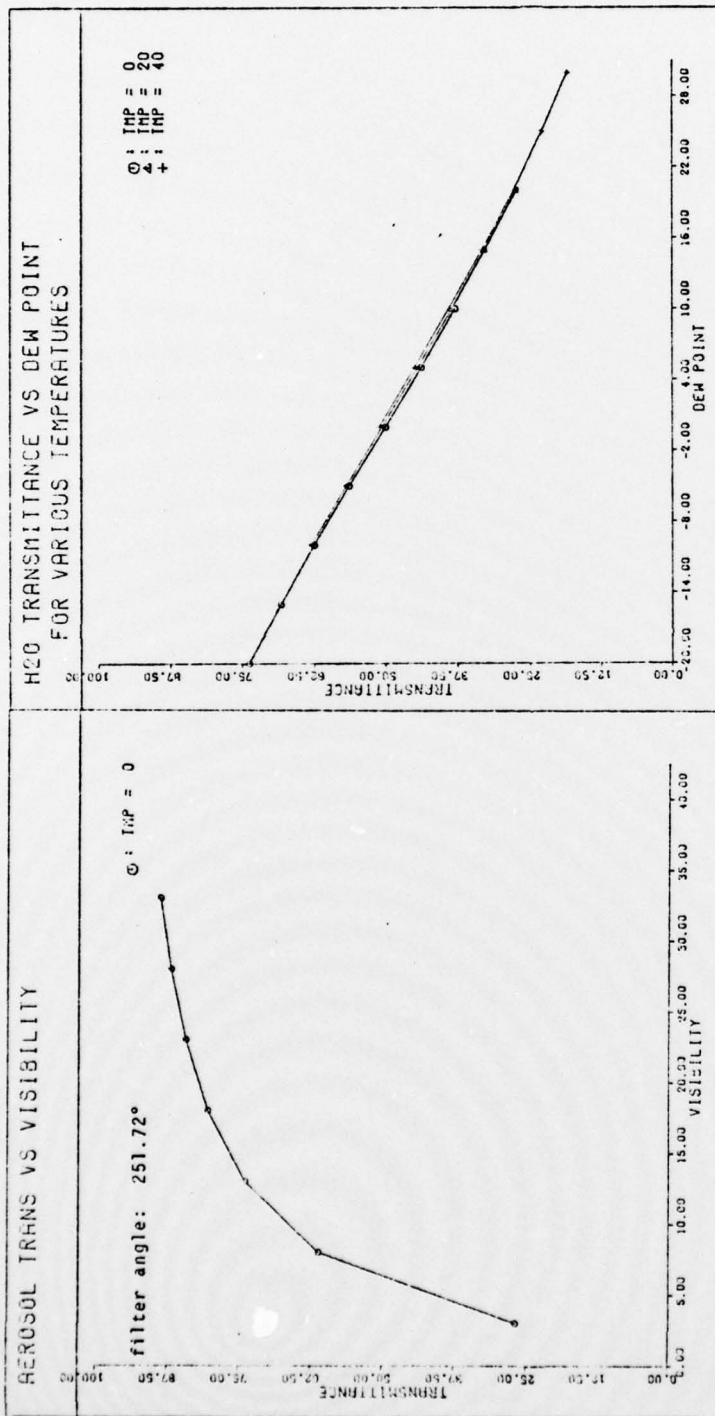


Fig. B6. 3.98 um Transmission as a Function of Visibility and Water Vapor Content

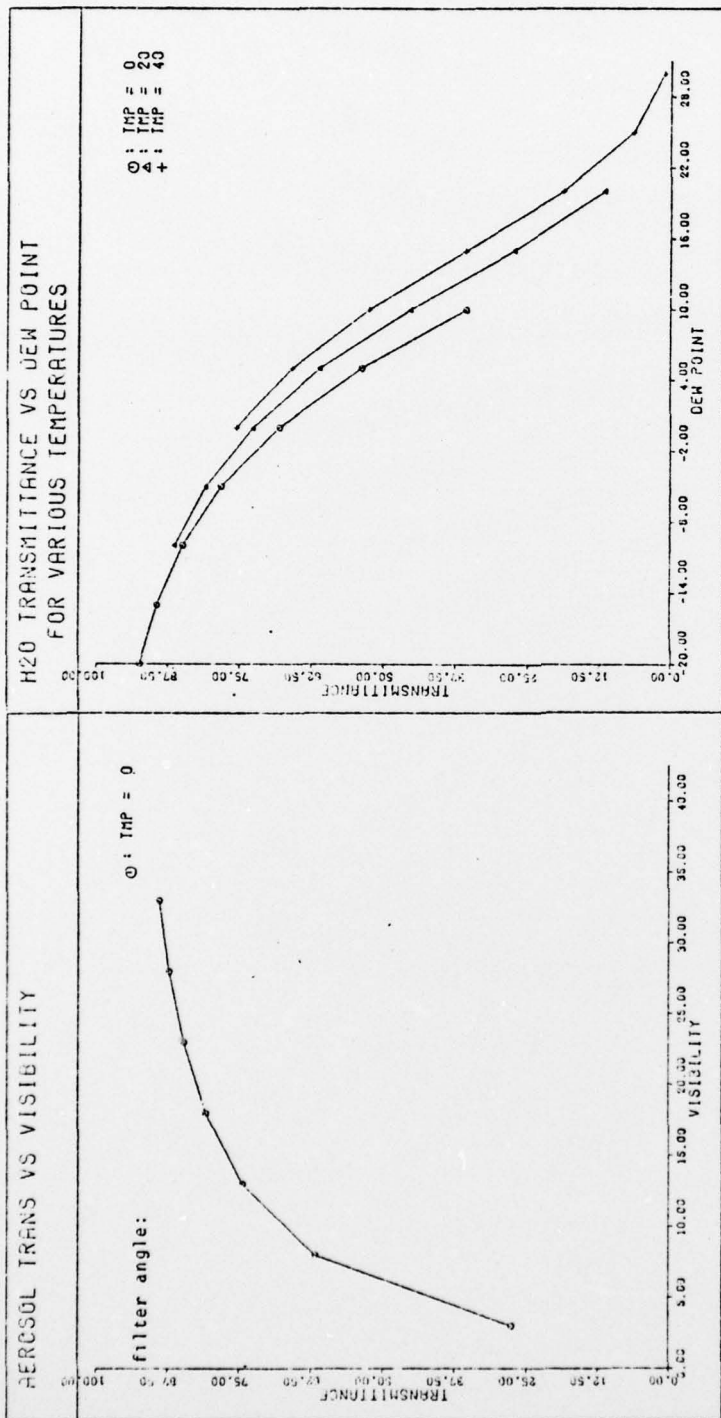


Fig. B7. 4.81  $\mu$ m Transmission as a Function of Visibility and Water Vapor Content

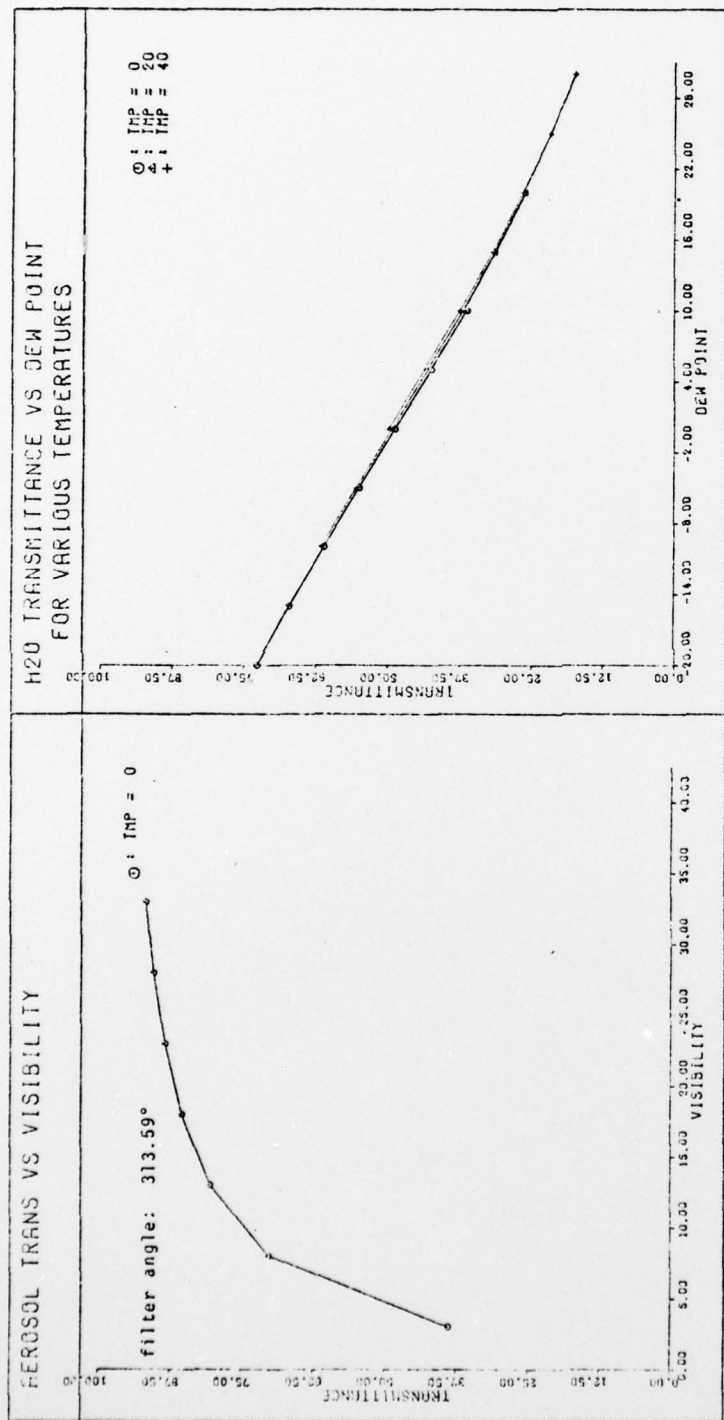


Fig. B8. 9.12 um Transmission as a Function of Visibility and Water Vapor Content

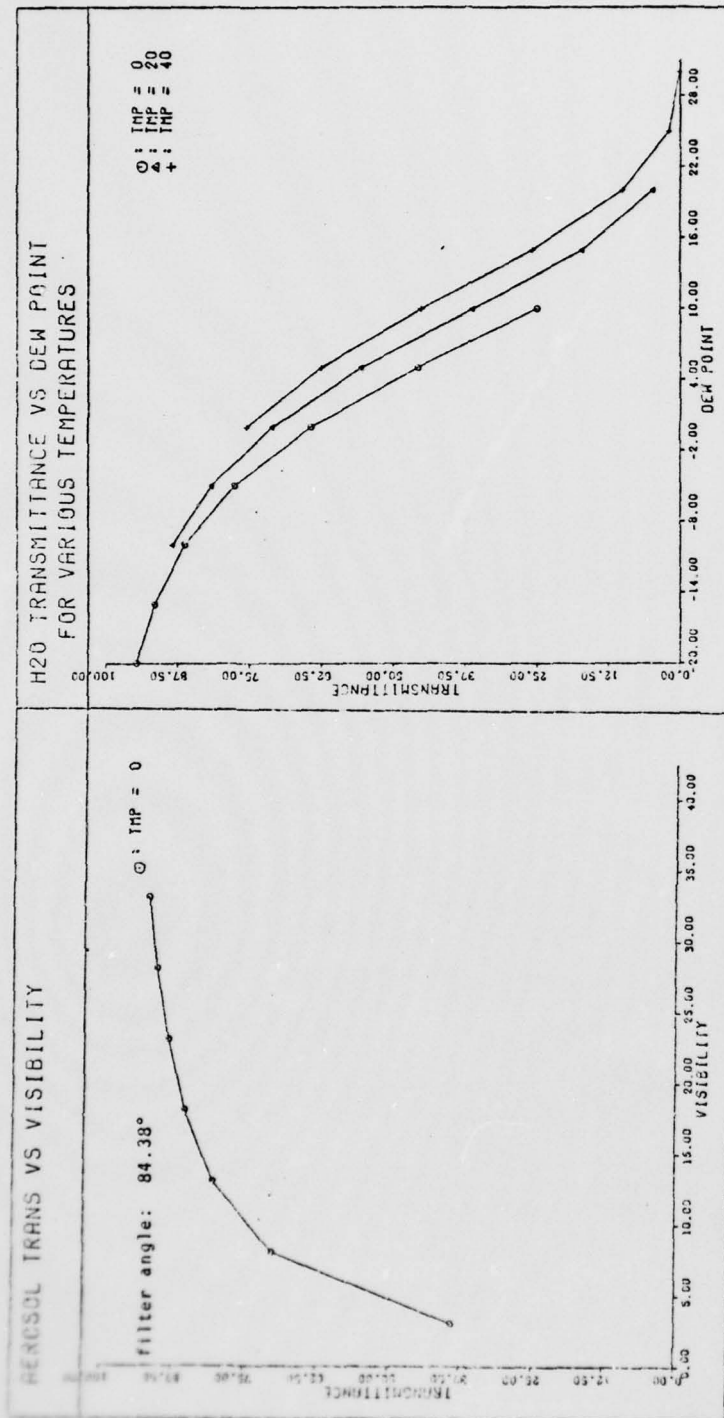


Fig. 89. 10.78 um Transmission as a Function of Visibility and Water Vapor Content

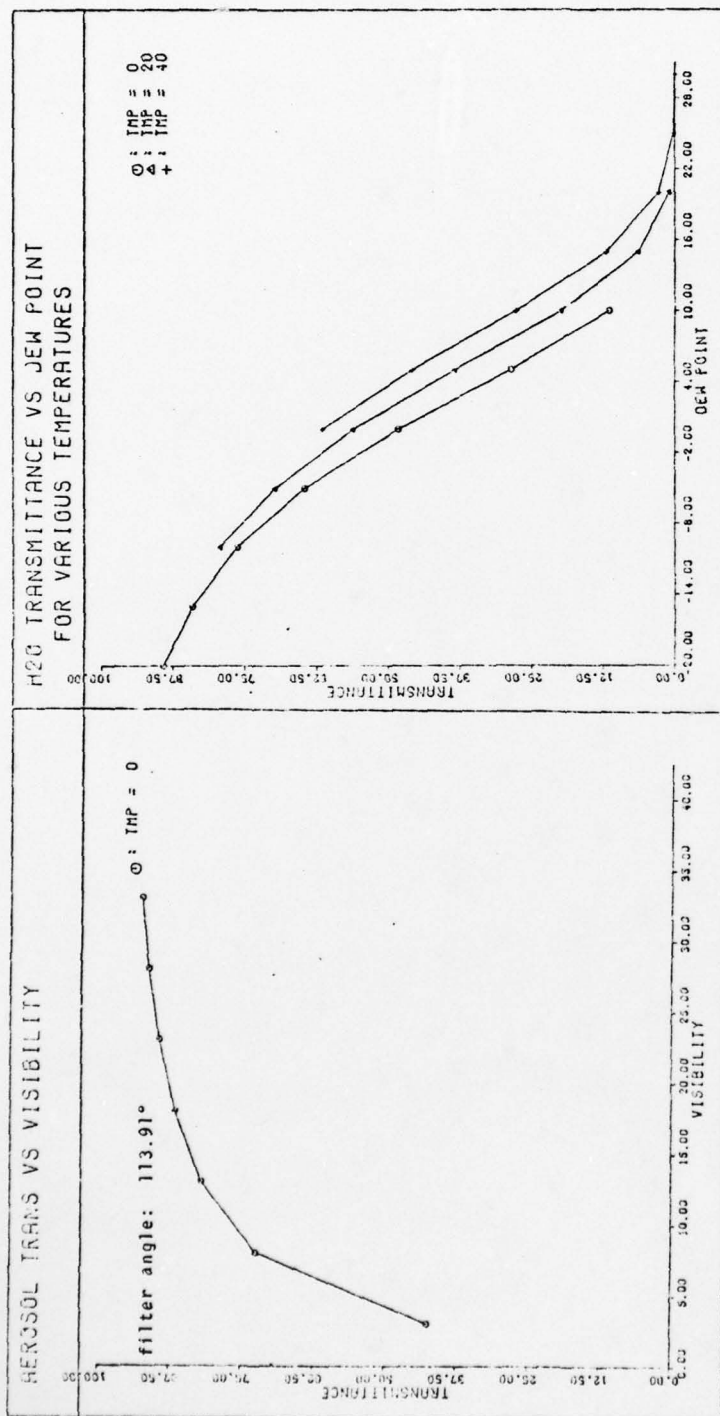


Fig. 810. 11.95 um Transmission as a Function of Visibility and Water Vapor Content

## VITA

Leo Owen Vroombout was born 6 September 1940 in Camden, New Jersey. He graduated from Merchantville High School in 1958 and attended Princeton University where he was awarded a Bachelor of Arts degree in Physics in 1962. After graduation, he attended AFROTC summer camp at Eglin AFB where he was commissioned on Friday, 13 July 1962. He began active duty in September, 1962 in the Aeronautical Systems Division (ASD), Wright-Patterson AFB, Ohio. After five years of developing and flight testing infrared and laser imaging systems, he was transferred to the Minuteman SPO, SAMSO at Norton AFB, CA. At Norton, he was the Reentry Vehicles Survivability/Vulnerability Staff Officer until he left active duty in May, 1969. He returned to ASD as a civil servant and continued his career as an electronics engineer responsible for developing infrared imaging systems. After participating in the combat evaluation of an infrared reconnaissance system in Southeast Asia, he began work for the Air Force Avionics Laboratory (AFAL) in 1973. At AFAL he became responsible for the Air Force Second Generation FLIR program and continued in that position until entering the School of Engineering, Air Force Institute of Technology, in June 1976.

Permanent address: 2802 Varsity Drive  
Fairborn, Ohio 45324

REPORT DOCUMENTATION PAGE		READ INSTRUCTIONS BEFORE COMPLETING FORM
1. REPORT NUMBER 14 AFIT/GEP/PH/77-14	2. GOVT ACCESSION NO.	3. RECIPIENT'S CATALOG NUMBER 9 Master's thesis
4. TITLE (and Subtitle) 6 LONG PATH, VISIBLE AND INFRARED TRANSMISSOMETER: CALIBRATION AND USE.	5. TYPE OF REPORT & PERIOD COVERED MS THESIS	
7. AUTHOR(s) 10 LEO [ ] /VROOMBOUT Owen	6. PERFORMING ORG. REPORT NUMBER	
9. PERFORMING ORGANIZATION NAME AND ADDRESS AIR FORCE INSTITUTE OF TECHNOLOGY (AFIT-EN) WRIGHT-PATTERSON AFB, OH 45433	8. CONTRACT OR GRANT NUMBER(s) 12 86p.	
11. CONTROLLING OFFICE NAME AND ADDRESS	10. PROGRAM ELEMENT, PROJECT, TASK AREA & WORK UNIT NUMBERS 16 62204F 17 05 20040553	
14. MONITORING AGENCY NAME & ADDRESS (if different from Controlling Office)	12. REPORT DATE 11 Oct 77	
	13. NUMBER OF PAGES 85	
	15. SECURITY CLASS. (of this report) Unclassified	
15a. DECLASSIFICATION/DOWNGRADING SCHEDULE		
16. DISTRIBUTION STATEMENT (of this Report) Approved for public release; distribution unlimited.		
17. DISTRIBUTION STATEMENT (of the abstract entered in Block 20, if different from Report)		
18. SUPPLEMENTARY NOTES APPROVED FOR PUBLIC RELEASE AFR 190-17. JERRAL F. GUESS, Captain, USAF Director of Information		
19. KEY WORDS (Continue on reverse side if necessary and identify by block number) Transmissometer Infrared transmission Atmospheric transmission		
20. ABSTRACT (Continue on reverse side if necessary and identify by block number) The Barnes Model 14-WP transmissometer is one of the principle optical path calibration instruments of the Air Force Avionics Laboratory's Targeting Systems Characterization Facility. A simple test based on LOWTRAN IIIB was devised to certify system calibration while installed on an eight kilometer optical path. In addition, an optical path anomaly was investigated. Results are discussed and recommendations for additional calibration tests and new procedures are made.		